Neuron
Primer

Optogenetics in Neural Systems

Ofer Yizhar,[1] Lief E. Fenno,[1] Thomas J. Davidson,[1] Murtaza Mogri,[1] and Karl Deisseroth[1,2,3,4,*]
[1]Department of Bioengineering
[2]Department of Psychiatry and Behavioral Sciences
[3]CNC Program
[4]Howard Hughes Medical Institute
Stanford University, Stanford, CA, 94305, USA
*Correspondence: deissero@stanford.edu
DOI 10.1016/j.neuron.2011.06.004

Both observational and perturbational technologies are essential for advancing the understanding of brain function and dysfunction. But while observational techniques have greatly advanced in the last century, techniques for perturbation that are matched to the speed and heterogeneity of neural systems have lagged behind. The technology of optogenetics represents a step toward addressing this disparity. Reliable and targetable single-component tools (which encompass both light sensation and effector function within a single protein) have enabled versatile new classes of investigation in the study of neural systems. Here we provide a primer on the application of optogenetics in neuroscience, focusing on the single-component tools and highlighting important problems, challenges, and technical considerations.

Introduction

Optogenetics, as the term has come to be commonly used, refers to the integration of optics and genetics to achieve gain- or loss-of-function of well-defined events within specific cells of living tissue (Deisseroth et al., 2006; Scanziani and Häusser, 2009; Deisseroth 2010, 2011). For example, microbial opsin genes can be introduced to achieve optical control of defined action potential patterns in specific targeted neuronal populations within freely moving mammals or other intact-system preparations. Interdisciplinary by nature, optogenetics requires (1) engineered control tools that can be readily targeted to specific cells, (2) technologies for light delivery, and (3) methods for integrating optical control with compatible readouts (such as fluorescent organic or genetically encoded activity indicators, electrical recording, fMRI signals, or quantitative behavioral analysis).

Aspects of the conceptual inspiration for optogenetics can be traced to the 1970s. In 1979 Francis Crick, taking note of the complexity of the mammalian brain and the fact that electrodes cannot readily distinguish different cell types (Crick, 1979), suggested that a major challenge facing neuroscience was the need to precisely control activity in one cell type while leaving the others unaltered. Crick later speculated in lectures that light might be a relevant control tool, but without a concept for how this could be done. Yet years earlier (in an initially unrelated line of research), bacteriorhodopsin had been identified (Oesterhelt and Stoeckenius, 1971, 1973) as a microbial single-component light-activated ion pump. Further work in thousands of papers over the ensuing decades led not only to deeper understanding of bacteriorhodopsin but also to the discovery of many new members of this microbial opsin family, which includes membrane-bound ion pumps and channels such as halorhodopsins (Matsuno-Yagi and Mukohata, 1977) and channelrhodopsins (Nagel et al., 2002) that transport various ions across the membrane in response to light (Matsuno-Yagi and Mukohata, 1977; Lanyi and Oesterhelt, 1982; Schobert and Lanyi, 1982; Béjà et al., 2000; Nagel et al., 2002, 2003; Ritter et al., 2008; Zhang et al., 2008).

It took decades for these two concepts to be brought together by neuroscientists, although microbial opsin genes were widely known and had long been understood to give rise to single-component light-activated regulators of transmembrane ion conductance. But there were fundamental caveats for those who considered such a possibility for optical neural control over the decades, including the presumption that photocurrents would be too weak and slow to control neurons efficiently, the presumption that microbial membrane proteins in fragile mammalian neurons would be poorly expressed or toxic, and most importantly the presumption that additional cofactors such as all-*trans* retinal (the separate organic light-absorbing chromophore employed by microbial opsins) would have to be added to any intact-tissue experimental system. These preconceptions (strikingly similar to those that slowed the development of green fluorescent protein) were all reasonable enough to deter experimental implementation, and efforts were therefore focused elsewhere. Yet in the summer of 2005 it was reported that introduction of a single-component microbial opsin gene into mammalian neurons (without any previously tested or other component) resulted in reliable sustained control of millisecond-precision action potentials (Boyden et al., 2005); many additional papers from work conducted contemporaneously appeared over the next year (Li et al., 2005; Nagel et al., 2005; Bi et al., 2006; Ishizuka et al., 2006). Moreover, while retinoids were already well known to be present in large quantities in embryonic tissues and in the retina, it was soon found that mature mammalian brains (Deisseroth et al., 2006; Zhang et al., 2006), and indeed all vertebrate tissues thus far examined (e.g., Douglass et al., 2008) contain sufficient all-*trans* retinal for microbial opsin genes to define a single-component strategy. By 2010 the major classes of ion-conducting microbial opsins (including bacteriorhodopsin, channelrhodopsin, and halorhodopsin) had all proven to function as optogenetic control tools in mammalian neurons, as described below.

Since earlier, multicomponent efforts for photosensitization of cells (for example, involving cascades of multiple genes or combinations of genes and custom organic chemicals (Zemelman et al., 2002, 2003; Banghart et al., 2004; Lima and Miesenböck, 2005; Kramer et al., 2005; Volgraf et al., 2006) have been recently reviewed (Gorostiza and Isacoff, 2008; Miesenböck, 2009), here we provide a primer focusing on single-component optogenetics, delineating guiding principles for scientific investigation and summarizing the enabling technologies for neuroscience application. However, most of the techniques developed for this approach (ranging from genetic targeting methods, to addressing experimental confounds, to intact-system light delivery methods) will be relevant to any biological system or optogenetic strategy. We do not attempt to review in any form the very large number of papers and results that have emerged in this field, nor to address every technique, reagent, and device linked to optogenetics. Rather, here we highlight limitations, challenges, and obstacles in the field and outline general principles for designing, conducting, and reporting optogenetic experiments.

Microbial Opsin Genes

Optogenetics is not simply photoexcitation or photoinhibition of targeted cells; rather, optogenetics must deliver gain or loss of function of precise events—just as in genetics, where single-gene manipulations are the core currency of the field. This means that in neuroscience, millisecond-scale precision is essential to true optogenetics, to keep pace with the known dynamics of the targeted neural events such as action potentials and synaptic currents. Moreover, this level of precision must be operative within intact systems including freely moving mammals. All strategies to achieve optical control, including those involving microbial opsin genes, initially displayed serious limitations in meeting this goal. The multicomponent character, longer-timescale temporal properties, and/or requirement for high-intensity UV light characteristic of the earlier strategies (Zemelman et al., 2002; Banghart et al., 2004; Lima and Miesenböck, 2005; Kramer et al., 2005) have limited adoption and application to mammalian and other systems, but single-component microbial opsin gene strategies also initially displayed problems as well ranging from inadequate control capability (Boyden et al., 2005; Gunaydin et al., 2010) to toxicity (Gradinaru et al., 2008, 2010; Zhao et al., 2008) to challenges linked to light delivery in vivo (Aravanis et al., 2007; Adamantidis et al., 2007). A long process of tool engineering and substantial development of enabling technologies was required over the next several years.

The key properties of these microbial optogenetic tools relate to the ecology of their original host organisms, which respond to the environment using seven-transmembrane proteins encoded by the type I class of opsin gene (Yizhar et al., 2011b). Type I opsins are protein products of microbial opsin genes and are termed rhodopsins when bound to retinal. However, in typical heterologous expression experiments the precise composition of retinoid-bound states is uncharacterized. Therefore in the setting of neuroscience application, the tools are conservatively referred to as opsins (a more accurate and convenient shorthand for common use, since only "opsin" correctly applies to the genes as well as to the protein products). These proteins are distinguished from their mammalian (type II) counterparts, in that they are single-component light-sensing systems; the two operations—light sensing and ion conductance—are carried out by the same protein.

The first identified, and still by far the best studied, type I protein is the haloarchaeal proton pump bacteriorhodopsin (BR; Figure 1A; Oesterhelt and Stoeckenius, 1971, 1973; Racker and Stoeckenius, 1974). Under low-oxygen conditions, BR is highly expressed in haloarchaeal membranes and serves as part of an alternative energy-production system, pumping protons from the cytoplasm to the extracellular medium to generate a proton-motive force to drive ATP synthesis (Racker and Stoeckenius, 1974; Michel and Oesterhelt, 1976). These light-gated proton pumps have since also been found in a wide range of marine proteobacteria as well as in other kingdoms of life, where they employ similar photocycles (Béjà et al., 2001; Váró et al., 2003) and have been hypothesized to play diverse roles in cellular physiology (Fuhrman et al., 2008).

A second class of microbial opsin genes encodes halorhodopsins (Figure 1A). Halorhodopsin (HR) is a light-activated chloride pump first discovered in archaebacteria (Matsuno-Yagi and Mukohata, 1977). The operating principles of halorhodopsin (HR) are similar to those of BR (Essen, 2002), with the two main differences being that halorhodopsin pumps chloride ions and its direction of transport is from the extracellular to the intracellular space. Specific amino acid residues have been shown to underlie the differences between BR and HR in directionality and preferred cargo ion (Sasaki et al., 1995). After initial identification of halorhodopsin, other members of this class soon followed; for example, Lanyi and colleagues expanded the family by identifying a halorhodopsin from *Natronomonas pharaonis* in 1982 (NpHR; Lanyi and Oesterhelt, 1982).

Next, a third class of conductance-regulating microbial opsin gene (channelrhodopsin or ChR) was identified (Figure 1A). Nagel and Hegemann demonstrated light-activated ion-flux properties (Nagel et al., 2002) for a protein encoded by one of the genomic sequences from the green algae *Chlamydomonas reinhardtii*, as Stoeckenius, Oesterhelt, Matsuno-Yagi, and Mukohata had earlier for the proteins halorhodopsin and bacteriorhodopsin. Subsequent papers from several groups described a second and third channelrhodopsin (Nagel et al., 2003; Zhang et al., 2008), and many more will follow. While ChR is highly homologous to BR, especially within the transmembrane helices that constitute the retinal-binding pocket, in channelrhodopsins the ion-conducting activity is largely uncoupled from the photocycle (Feldbauer et al., 2009); an effective cation channel pore is opened, which implies that ion flux becomes independent of retinal isomerization and rather depends on the kinetics of channel closure. In neurons, net photocurrent due to ChR activation is dominated by cation flow down the electrochemical gradient (resulting in depolarization), rather than by the pumping of protons. Like the BRs and HRs, ChRs from various species (Nagel et al., 2002; Zhang et al., 2008) are functional in neurons with a range of distinct and useful intrinsic properties.

The single-component optogenetic palette available to neuroscientists now contains tools for four major categories of fast excitation, fast inhibition, bistable modulation, and control of intracellular biochemical signaling in neurons and other cell

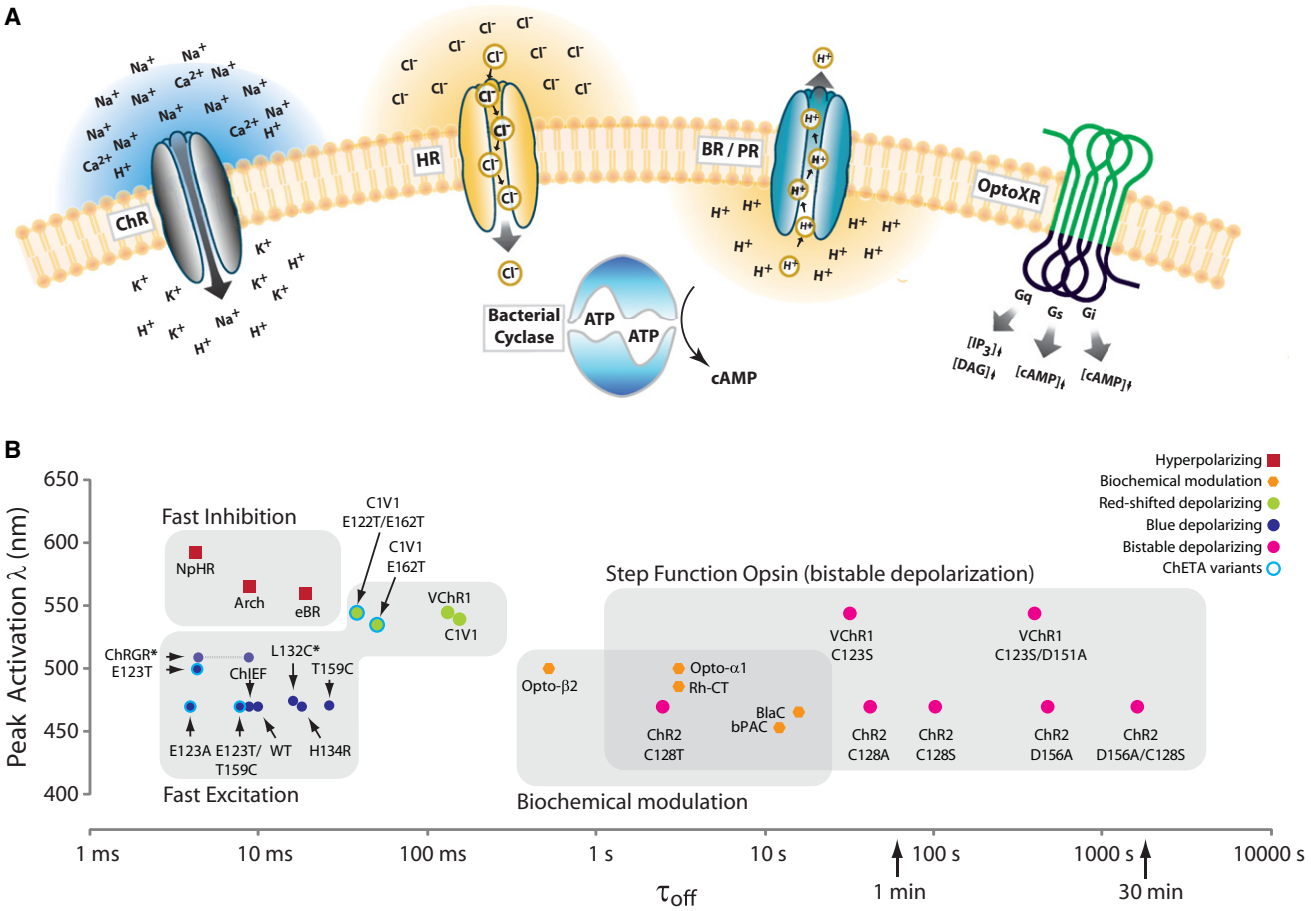

Figure 1. Basic Properties of Known Single-Component Optogenetic Tools with Published Spectral and Kinetic Information

(A) Single-component optogenetic tool families; transported ions and signaling pathways are indicated.

(B) Kinetic and spectral attributes of optogenetic tool variants for which both of these properties have been reported and for which minimal activity in the dark is observed. Visible spectrum shown; not venturing into the ultraviolet is preferred, for safety and light penetration reasons, although the 450–470 nm peak probes also can be excited very effectively with UV light (~360–390 nm). Decay kinetics are plotted against peak activation wavelength only to demonstrate groupings and classes over the range of spectral and temporal characteristics and the feasibility of dual channel control using tools that are well separated in the spectral and temporal domains; see Table 1 for additional information and references. Kinetic data are not published for the proton pump Mac but the Mac action spectrum peak ~565 nm is identical to that of Arch (Chow et al., 2010). Opto-XR kinetics were obtained in vivo and should be taken only as an upper bound since the assay involved a downstream measure (spiking). Decay kinetics are temperature dependent; all other reported values except ChRGR are recorded at RT, with ~50% decrease in τ_{off} expected at 37C. *Since ChRGR has only been studied at elevated (34°C) T, we denote likely RT range for ChRGR shifted to the right. Values for channelrhodopsin/fast receiver and channelrhodopsin/wide receiver (Wang et al., 2009) can be estimated at 7 and 14 ms, respectively; these are not shown but respond at 470 nm and have not yet been functionally validated in neurons. L132C (CatCH) τ_{off} value was not measured in neurons, and its properties may depend on other channels in the host cell as well as the host cell tolerance of, and response to, higher levels of elevated intracellular Ca^{2+} (Kleinlogel et al., 2011).

types (Figure 1B, Table 1). This array of optogenetic tools, the result of molecular engineering and genomic efforts, allows experimental manipulations tuned for (1) the desired physiologic effect; (2) the desired kinetic properties of the light-dependent modulation; and (3) the required wavelength, power, and spatial extent of the light signal to be deployed.

Fast Optogenetic Excitation for Neuroscience

Microbial opsin genes in some cases lead to expression of light-inducible photocurrents when introduced into neurons, but to date, optogenetic application of all of these genes has benefited substantially from molecular modification. In neuroscience, after initial demonstration (Boyden et al., 2005; Li et al., 2005; Nagel et al., 2005; Bi et al., 2006; Ishizuka et al., 2006), a subsequent widely used form of channelrhodopsin was generated by substituting mammalian codons to replace algal codons in order to achieve higher expression levels (humanized ChR2 or hChR2; Zhang et al., 2006; Adamantidis et al., 2007; Aravanis et al., 2007; Zhang et al., 2007), and this process is now typically applied to all new opsin genes. An important caveat is that codon optimization and mutagenesis can lead to unanticipated effects in different experimental systems, and an intervention that gives rise to improved properties in mammalian neurons (such as point mutation, codon optimization or membrane trafficking modification) could in principle show impairment in other properties (and unchanged or even impaired performance in another cell or system). For example, introduction of the H134R mutation into ChR2 was found to be of mixed impact, improving currents ~2-fold during prolonged stimulation

Table 1. Single-Component Optogenetic Tools with Both Spectral and Kinetic Data Published

Opsin	Mechanism	Peak Activation λ	Off Kinetics (τ, ms)*	Kinetics References
Blue/Green Fast Excitatory				
ChR2	Cation channel	470 nm	~10 ms	Boyden et al., 2005; Nagel et al., 2003
ChR2(H134R)	Cation channel	470 nm	18 ms	Nagel et al., 2005; Gradinaru et al., 2007
ChR2 (T159C)	Cation channel	470 nm	26 ms	Berndt et al., 2011
ChR2 (L132C)	Cation channel	474 nm	16 ms*	Kleinlogel et al., 2011
ChETAs: ChR2(E123A) ChR2(E123T) ChR2(E123T/T159C)	Cation channel	470 nm (E123A) 490 nm (E123T)	4 ms (E123A) 4.4 ms (E123T) 8 ms (E123T/T159C)	Gunaydin et al., 2010; Berndt et al., 2011
ChIEF	Cation channel	450 nm	~10 ms	Lin et al., 2009
ChRGR	Cation channel	505 nm	4-5 ms* (8-10ms)	Wang et al., 2009; Wen et al., 2010
Yellow/Red Fast Excitatory				
VChR1	Cation channel	545 nm	133 ms	Zhang et al., 2008
C1V1	Cation channel	540 nm	156 ms	Yizhar et al., 2011a
C1V1 ChETA (E162T)	Cation channel	530 nm	58 ms	Yizhar et al., 2011a
C1V1 ChETA (E122T/E162T)	Cation channel	535 nm	34 ms	Yizhar et al., 2011a
Bistable Modulation				
ChR2-step function opsins (SFOs)	Cation channel	470 nm activation / 590 nm deactivation	2 s (C128T); 42 s (C128A) 1.7 min (C128S) 6.9 min (D156A) 29 min (128S/156A)	Berndt et al., 2009; Bamann et al., 2010 Yizhar et al., 2011a
VChR1-SFOs	Cation channel	560 nm activation / 390 nm deactivation	32 s (C123S) 5 min (123S/151A)	
Yellow/Red Inhibitory				
eNpHR3.0	Chloride pump	590 nm	4.2 ms	Gradinaru et al., 2010
Green/Yellow Inhibitory*				
Arch/ArchT	Proton pump	566 nm	9 ms	Chow et al., 2010
eBR	Proton pump	540 nm	19 ms	Gradinaru et al., 2010
Biochemical Modulation				
Opto-β2AR	↑ G_s-protein signaling	500 nm	0.5 s	Airan et al., 2009
Opto-α1AR	↑ G_q-protein signaling	500 nm	3 s	Airan et al., 2009
Rh-CT(5-HT1A)	↑ $G_{i/o}$-protein signaling	485 nm	3 s	Oh et al., 2010
bPAC	↑ cAMP	453 nm	12 s	Stierl et al., 2011
BlaC	↑ cAMP	465 nm	16 s (50% decay)	Ryu et al., 2010

* Decay kinetics are temperature dependent; values were taken from or estimated from published traces where available and necessary. Opto-XR kinetics were obtained in vivo and should be taken only as an upper bound since the assay involved a downstream measure (spiking). All other reported values except ChRGR are recorded at RT, with ~50% decrease in τ_{off} expected at 37°C; since ChRGR has only been studied at elevated (34°C) T, we denote likely RT range for ChRGR in parentheses. Values for channelrhodopsin/fast receiver and channelrhodopsin/wide receiver (Wang et al., 2009) were estimated at 7 and 14 ms, respectively, at 34°C; these are not shown but respond at 470 nm and have not yet been functionally validated in neurons. Kinetic data are not published for the proton pump Mac but the Mac action spectrum peak ~565 nm is similar to that of Arch (Chow et al., 2010). L132C (CatCH) τ_{off} value was not measured in neurons, and its properties may depend on other channels in the host cell as well as the host cell tolerance of, and response to, higher levels of intracellular Ca^{2+} (Kleinlogel et al., 2011).

although at the expense of ~2-fold slower channel-closure kinetics and consequent poorer temporal precision (Nagel et al., 2005; Gradinaru et al., 2007); nevertheless, like hChR2, hChR2(H134R) can drive precise low-frequency spike trains within intact tissue and is widely used. Similarly, modification of the Thr159 position (T159C; Berndt et al., 2011) and the Leu132 position (L132C; Kleinlogel et al., 2011) were found to increase photocurrent magnitude with a concomitant slowing

in channel off-kinetics. Notably, modified ChRs have been developed with a chimera-based approach (Wang et al., 2009; Lin et al., 2009; Yizhar et al., 2011a), resulting in both quantitatively stronger photocurrents and reduced desensitization in cultured neurons.

A substantially red-shifted channelrhodopsin (VChR1) that can be excited by amber (590 nm) light, which does not affect ChR2 at all, was identified by genomic strategies and validated in cultured neurons (Zhang et al., 2008), raising the possibility of combinatorial excitation in vivo (Yizhar et al., 2011a). Most channelrhodopsins described to date have a relatively low single-channel conductance and broad cation selectivity (Nagel et al., 2003; Zhang et al., 2008; Lin et al., 2009; Tsunoda and Hegemann, 2009; Gunaydin et al., 2010), but cellular photocurrents can be vastly improved with molecular engineering strategies, including for VChR1 (e.g., Yizhar et al., 2011a). With the exception of the recently reported L132C mutant (Kleinlogel et al., 2011), channelrhodopsins generally give rise to only small Ca^{2+} currents at physiological Ca^{2+} concentrations, and increases in cytosolic Ca^{2+} due to channelrhodopsin activation result chiefly from activation of endogenous voltage-gated Ca^{2+} channels via membrane depolarization and neuronal spiking (Zhang and Oertner, 2007), which also occur to varying extents with different native depolarization processes. Second- and also third-order conductances (e.g., Ca^{2+}-gated potassium and chloride currents) must nevertheless be kept in mind, especially when higher Ca^{2+}-conducting channelrhodopsins are employed, as these will influence light-evoked activity in a manner that may vary from cell type to cell type; for example, different cells (or even different regions of the same cell) may elicit, tolerate, or respond to higher levels of Ca^{2+} differently. Recent modeling work in which photocurrent responses were integrated with a Hodgkin-Huxley neuron model (Grossman et al., 2011) will be potentially expandable to include these second-order conductances and predict cellular responses under various stimulation paradigms.

Bistable behavior has been obtained with molecular engineering of ChRs, generating a distinct class of opsin-based tools in which mutations in cysteine-128 and aspartate-156 in ChR2 significantly prolong the photocycle (Berndt et al., 2009; Bamann et al., 2010). While the conductance of wild-type ChR2 deactivates with a time constant of ~10 ms upon light cessation, the ChR2(C128X) mutants are vastly slower. For example, in the C128T, C128A, and C128S mutants, photocurrents decay spontaneously with time constants of 2 s, 42 s, and ~100 s, respectively (Berndt et al., 2009). Termination of this stable blue-light triggered photocurrent is still possible by applying a pulse of yellow light (560–590 nm; Berndt et al., 2009). Mutant genes of this class are termed step-function opsin (SFO) genes, since they enable bistable, step-like control of neuronal membrane potential that can bring cells closer to action potential threshold and increase the probability of spiking to endogenous synaptic inputs (Berndt et al., 2009). Two crucial distinct properties of SFOs by comparison with conventional ChRs are (1) orders-of-magnitude increased effective cellular light sensitivity, which results from accumulation of open channels during the light pulse, leading to larger volumes of tissue recruited in vivo for a given light intensity (Berndt et al., 2009; Diester et al., 2011); and (2) the asynchronous nature of SFO-mediated neuronal activation, which does not entrain all the expressing neurons into a single pattern dictated by light delivery (Berndt et al., 2009), a property that may be preferable in some applications (but not in others requiring synchronous or precisely timed spikes).

SFOs have recently been shown to deliver bistable optogenetic control in *C. elegans* neurons and muscle cells (Schultheis et al., 2011) and in the brains of awake, behaving primates (Diester et al., 2011). Additional and combinatorial mutagenesis based on these initial principles has led to additional SFOs (Bamann et al., 2010; Yizhar et al., 2011a), with time constants of deactivation up to 30 min (Yizhar et al., 2011a). With these stabilized SFOs, targeted neurons can in principle be "stepped" to a stable depolarized resting potential, which could be followed by removal of the light source and initiation of behavioral or physiological experimentation in the complete absence of light or other hardware. Moreover, the use of long low-intensity light pulses (in the setting of the steady photon-integration properties of cells expressing the stable SFOs) could allow elimination of variability of recruitment of cells in vivo attributable to variations in light intensity experienced, since the full population of opsin-expressing cells even in a large volume of tissue could be brought to saturating photocurrent levels over time.

While these tools afford experimental opportunities, an important caveat of this approach is that it must be validated in each system to quantify the effect on targeted cells. The published SFOs have slower activation kinetics that do not tend to directly elicit spikes or drive neurons into a state of depolarization block (the latter of which could give rise to a paradoxical inhibition rather than excitation of the targeted cells), but studies involving SFOs (indeed involving any optogenetic intervention) should still be accompanied by electrophysiological validation at the corresponding experimental time point (matching opsin expression levels) so that the effect on the targeted cell and tissue may be understood for proper interpretation of experimental results. Here, the SFOs, and indeed all optogenetic tools, offer a class of validation not typically possible with electrical stimulation, since with electrical stimulation it remains unclear precisely how the targeted region is responding due to the difficulties associated with electrical recording in the setting of electrical stimulation artifacts.

None of the ChRs described above were initially shown to directly evoke reliable spiking above 40 Hz, while many neuronal cell types and physiological processes involve or require high-frequency spike trains (>40 Hz). Even the seemingly fast off-kinetics of wild-type ChR2 (τ ~10 ms), and certainly those of H134R (τ ~20 ms), are insufficient for precise control at high spike rates, a phenomenon that may be compounded by the further depolarization-dependent slowing of deactivation observed for most ChRs (Berndt et al., 2011). An important group of relevant neurons are the fast-spiking inhibitory parvalbumin-expressing interneurons, which in cortex are thought to be involved in generation of oscillatory rhythms and synchronization across brain regions (Freund, 2003). Activation of these neurons with wild-type ChR2 is not sufficiently precise above 40 Hz, due to spike doublets, plateau potentials, and temporal nonstationarity in the form of missed spikes late in sustained high-frequency light pulse trains (which may result from the failure of full membrane repolarization and consequent insufficient

voltage-dependent deinactivation of voltage-gated sodium channels; Gunaydin et al., 2010).

Modifying ChR2 residue glutamate 123 to threonine or alanine (T/A) was found to accelerate channel closure kinetics from ~10 ms to ~4 ms, at the expense of moderately decreased photocurrent magnitude, a change that significantly increased the fidelity of fast optogenetic control (Gunaydin et al., 2010). These E123 variants can be combined with other modifications such as the H134R or T159C mutations (Gunaydin et al., 2010; Berndt et al., 2011) or membrane trafficking modifications (Gradinaru et al., 2008, 2010; Zhao et al., 2008). The E123 mutations appear unique thus far among channelrhodopsin mutations as they eliminate the sensitivity of channel kinetics to membrane potential, whether alone or in combination with other mutations (H134R and T159C; Berndt et al., 2011). Once this nonlinear and nonstationary effect is eliminated, the channel response to a light pulse can be more predictable and easier to model. These fast variants therefore address many dimensions of signal fidelity that are degraded with high frequency stimulation in wild-type ChR2. Opsins of this class (E123 mutations alone or in combination with other modifications; Gunaydin et al., 2010) are termed ChETAs (*Ch*R *E*123*T*/*A*). Notably, fast-spiking activity is not unique to the parvalbumin-expressing neurons, as many neuron types in the brain can fire at > 40 Hz; moreover, not only fast-spiking cells may benefit from ChETA usage, as the reduced occurrence of extra spikes (along with reduced spurious prolonged depolarizations) with ChETA can enhance the fidelity of evoked neural codes even in non-fast-spiking cells. ChETA tools have been shown to deliver improved performance within intact mammalian brain tissue (Gunaydin et al., 2010), while at the same time, a major caveat is that faster deactivation tends to translate into reduced effective cellular light sensitivity for long pulses of light, since fewer channels remain or accumulate in the open (conducting) state.

Pharmacological, optogenetic, and electrical stimulation will appear different (by comparison with native synaptic drive) to the directly targeted cells at the site of stimulation, since conductance changes, ion fluxes, and membrane potential changes will not originate precisely at the physiological pattern of synapses or receptor sites (although dendritic opsin targeting strategies may be relevant here; Gradinaru et al., 2007; Greenberg et al., 2011), nor be necessarily timed at physiological intervals relative to other events and cellular responses such as spiking. Any of these methods could also affect intracellular membranes (such as the endoplasmic reticulum, nuclear membranes, synaptic vesicles, and mitochondria). This concept must be kept in mind when experimental stimulation methods are used to study processes within single cells, more so than in the increasingly common study of downstream (postsynaptic) circuit or systems-level questions. Moreover, while optogenetic activation represents an important advance over electrical stimulation in its specificity, certain fundamental differences between optogenetic and electrical activation should be taken into consideration (Gradinaru et al., 2009; Llewellyn et al., 2010; Diester et al., 2011). Consider two equivalent experiments, one using electrical microstimulation of a targeted region in vivo, and another in which a channelrhodopsin gene is expressed in local neurons while an optical fiber is placed above the structure. Both types of stimulation will lead to action potentials in the targeted region. In the optogenetic experiment, the targeted cells and their axons will first be selectively activated, importantly followed by activation of synapses, cells, and circuits that are connected downstream of the targeted cells; moreover, when photosensitive axons are directly illuminated as in a projection-targeting experiment, smaller-caliber fibers are likely to be recruited at the lowest stimulation levels before larger-caliber fibers (orderly or physiological recruitment; Llewellyn et al., 2010). In contrast, the electrical experiment may first lead to spiking in diverse local, afferent, and passing axonal fibers (recruiting larger-caliber axons first in the phenomenon of recruitment reversal, with associated orthodromic and antidromic propagation even to nonlocal somata; Histed et al., 2009; Llewellyn et al., 2010), a property that may explain aspects of electrical deep brain stimulation (DBS) function in the treatment of Parkinson's Disease (Gradinaru et al., 2009) as well as microstimulation function in systems neuroscience.

While the specificity of optogenetics presents an opportunity to understand precisely how cells and circuits give rise to nervous system function, experimental effects will depend on the type of neuron and cellular compartment targeted as well as the stimulation parameters employed (pulse frequency, duration, amplitude, and other factors, just as with electrical stimulation). Moreover, opsin choice (e.g., ChETA versus H134R or L132C) could affect the extent to which paired-pulse or plasticity effects are elicited in a manner distinct from electrical stimulation, especially in experiments where light is directly applied to the axons and the ChR therefore directly influences presynaptic terminal ion flux; in contrast, where light is delivered directly to the soma and propagating sodium action potentials are generated, the resulting presynaptic bouton (and downstream postsynaptic) spikes may look indistinguishable from those generated by native electrical spike generation mechanisms in terms of ion flux and kinetics.

Fast Optogenetic Inhibition for Neuroscience

It must be recognized that delivering gain of function with a targeted channelrhodopsin only demonstrates that a particular pattern of activity in a defined population is causally sufficient for a circuit or behavioral property. But in principle multiple different cell populations could give rise to the same circuit or behavioral property, not necessarily only the cells that normally give rise to the effect in a naturalistic or physiological setting for the organism. For this reason, loss-of-function (inhibitory) tools are also important in optogenetics, for testing necessity of activity in the targeted cell population.

In a screen for hyperpolarizing fast optogenetic tools, the halobacterial HR (which gives rise to electrogenic chloride influx) showed excessive desensitization (Zhang et al., 2007). However, the homologous gene from *Natronomonas pharaonis* (NpHR; Lanyi and Oesterhelt, 1982; Scharf and Engelhard, 1994; Sato et al., 2005) gave rise to suitably stable outward (hyperpolarizing) currents (Zhang et al., 2007) with photocurrent peak ~590 nm (a wavelength at which ChR2 shows no response at all, enabling independent activation of ChR2 and NpHR to bidirectionally modulate activity; Figure 1). Unlike the excitatory channelrhodopsins, NpHR is a true pump and requires constant light in order to move through its photocycle. Moreover, although

optogenetic inhibition with NpHR was shown to operate well in freely moving worms and in mammalian brain slices (Zhang et al., 2007) as well as cultured neurons (Zhang et al., 2007; Han and Boyden, 2007), several years passed before mammalian validation of any inhibitory optogenetic tool was obtained by successful application to behavioral studies in intact mammals (Witten et al., 2010; Tye et al., 2011), due to membrane trafficking problems that required additional engineering (Gradinaru et al., 2008, 2010; Zhao et al., 2008).

At high expression levels, NpHR-EYFP-expressing cells were found to show accumulations of intracellular fluorescence that colocalized with endoplasmic reticulum (Gradinaru et al., 2008). Addition of an ER export motif from the Kir2.1 potassium channel (ER2—identified after a screen of many possible corrective motifs; Gradinaru et al., 2008) improved the surface membrane localization of NpHR and yielded eNpHR2.0 (Gradinaru et al., 2008; Zhao et al., 2008), with higher currents suitable for use in intact rodent tissue (Sohal et al., 2009; Tønnesen et al., 2009) as well as in human and nonhuman primate tissue (Busskamp et al., 2010; Diester et al., 2011). Next, eNpHR3.0, which additionally contains a neurite trafficking sequence from the Kir2.1 potassium channel, showed further enhanced photocurrents (nanoampere scale at moderate light intensities, < 5 mW/mm^2) that can be used to drive inhibition by yellow- or far-red-shifted wavelengths (up to 680 nm at the infrared border; Gradinaru et al., 2010).

eNpHR3.0 ultimately enabled the loss-of-function side of optogenetics for behavior in freely moving mammals (Witten et al., 2010; Tye et al., 2011), complementing the engineered channelrhodopsins that had enabled gain-of-function in freely moving mammals (Adamantidis et al., 2007). eNpHR3.0 was first used along with bilateral optical fiber devices to inhibit the cholinergic neurons of the nucleus accumbens and elucidate a causal role for these rare cells in implementing cocaine conditioning in freely moving mice, which appears to operate via enhancing inhibition of inhibitory striatal medium spiny neurons (Witten et al., 2010). eNpHR3.0 was also used in a two-fiber approach to inhibit a specific intra-amygdala projection in freely moving mice, implicating a defined neural pathway in aspects of anxiety and anxiolysis (Tye et al., 2011). Given the highly redundant and parallel architecture of neural circuitry, in general it may be more challenging to elicit loss-of-function than gain-of-function circuit effects; indeed, for loss-of-function experiments, as in these two studies, it is advisable to employ bilateral fibers to target corresponding structures in both hemispheres, rather than the single unilateral fiber in each test subject that typically suffices for gain-of-function work. These studies also depend on photocurrent stability of inhibitory opsin function on mammalian behavioral timescales.

The crystal structure of NpHR has been published (Kouyama et al., 2010) and illustrates that this protein has a high degree of structural homology within the retinal binding pocket with the proton pumps such as bacteriorhodopsin. In 2010 two groups explored the use of proton pumps (Mac, Arch, and eBR) as optogenetic tools (Chow et al., 2010; Gradinaru et al., 2010), finding robust efficacy but leaving open questions of long-term tolerability and functionality of proton-motive pumps in mammalian neurons. One caveat is the extent to which pumping of large proton fluxes to the extracellular space (especially in juxtamembranous compartments difficult to assess) might have unwanted or non-cell-type-specific effects; such an effect might manifest only under conditions where many (but not all) local neurons are expected to be opsin expressors, and might be detected in this case (e.g., in extracellular recordings) as optogenetic inhibition of spiking in nonexpressing cells with a slower mean timecourse than expected from the millisecond-scale kinetics of the pumps. Indeed, the inhibitory pumps (including chloride pumps) are typically driven with continuous light (to avoid rebound excitation), which could deter recovery of ionic or pH imbalances; in contrast, channelrhodopsins are permeant to cations including protons but are driven most typically in neuroscience experiments by well-separated pulses of light.

Finally, caution must be exercised, particularly with steady light, to avoid heating of tissue. It is therefore important to consider the light intensities required for optogenetic inhibition at a particular photocurrent value, keeping in mind that to compensate for scattering losses, in vivo light is typically delivered to the tissue at 100-fold or more higher intensity than required at the target cell (Aravanis et al., 2007; Gradinaru et al., 2010). To avoid toxicity while maintaining efficacy, we recommend selecting inhibitory opsins that allow delivery of $>$ 400 pA of current at irradiance values of $<$ 10–20 mW/mm^2 at the target cell, and we return to the issue of heating and irradiance levels below. While nanoampere-scale inhibitory currents sufficient for mammalian behavioral effects already can be recruited at < 5 mW/mm^2 (Gradinaru et al., 2010), ongoing engineering and discovery of known and existing opsins will continue to expand the optogenetic toolkit in this direction as well. Just as with NpHR as described above, modifying Arch by providing the ER2 motif for endoplasmic reticulum export—initially found by Gradinaru et al. (2008) and Zhao et al. (2008) to promote microbial opsin expression and function in neurons—allows generation of larger proton currents (J. Mattis, personal communication), and this membrane trafficking modification principle thus far appears to be a generalizable means (Gradinaru et al., 2010) by which heterologous membrane expression of novel microbial opsins for optogenetics in neuroscience may be achieved. Moreover, diverse opportunities to develop or discover new optogenetic tools exist given the large diversity of microbial opsin genes in nature, and since 2008 screens of genomic data have led to identification of many additional tools (e.g., Zhang et al., 2008; Chow et al., 2010; Gradinaru et al., 2010; Yizhar et al., 2011a).

Tools for Modulation of Biochemical Signaling

The microbial (type I) opsin genes described above encode strictly ion flow modulators, which control the excitability of a neuron by directly manipulating its membrane potential—either bringing the membrane potential nearer to or above the threshold for generating an action potential or hyperpolarizing the cell and thereby inhibiting spiking. While this approach has advantages of speed and precision, in some experimental protocols temporally precise modulation of intracellular processes may be necessary.

Vertebrate rhodopsin (such as the light-sensing protein in the mammalian eye) is both an opsin (type II), in that it is covalently bound to retinal (in the *cis* configuration) with function modulated

by the absorption of photons, and a G protein-coupled receptor (GPCR), in that it is coupled on the intracellular side to G protein signaling. Expressing vertebrate rhodopsins alone can confer light sensitivity, which can be observed as a slow inhibitory (Li et al., 2005) or excitatory (Melyan et al., 2005) modulation. Since these heterologous expression experiments are conducted in the absence of the native G protein (e.g., transducin), the rhodopsin must engage in novel interactions with unknown G proteins not normally linked to rhodopsin that are present in the host cell, and effects on cellular properties may therefore depend on the specific G protein pathways present in each host cell type. Optogenetic recruitment of well-defined biochemical signaling events can be achieved in generalizable fashion by constructing chimeras (Kim et al., 2005) between vertebrate rhodopsin and conventional ligand-gated GPCRs that can serve as single-component neural control tools (Airan et al., 2009; Oh et al., 2010), such as the dopaminergic, serotonergic, and adrenergic receptors that play important roles in neurotransmission and neuromodulation. This type II approach can capitalize upon the retinoids present within vertebrate tissues, as identified in the course of microbial (type I) opsin work (Deisseroth et al., 2006; Zhang et al., 2006). When used as optogenetic tools these type II fusion proteins are referred to as optoXRs, which allow for optically controlled intracellular signaling with temporal resolution suitable for modulating behavior in freely moving mice (Airan et al., 2009).

The speed and cellular precision that define biochemical optogenetic techniques, as with electrical optogenetic techniques, provide opportunities not achievable with pharmacological and genetic tools. Moreover, optoXRs (Airan et al., 2009) can leverage the optical interfaces (laser diode-fiberoptic devices; Aravanis et al., 2007) previously developed for type I work in freely moving mammals. Indeed, control of biochemical signaling represents an active and rapidly growing domain of optogenetics. Optical control over small GTPases has been described in cultured cells by several different laboratories (Levskaya et al., 2009; Wu et al., 2009; Yazawa et al., 2009) using optically modulated protein-protein interactions. Finally, microbial adenylyl cyclases have been recently described with lower dark activity than earlier microbial cyclases, and since they employ a flavin chromophore native to vertebrate tissues, these tools appear suitable for single-component optogenetic control (Ryu et al., 2010; Stierl et al., 2011). While these newer tools have not yet been shown to display single-component functionality in freely moving mammals, such capability is expected in systems where the required chromophores are present. Together, these experiments have extended optogenetic capability to essentially every cell type (even nonexcitable cells) in biology, and have successfully leveraged optical hardware and targeting techniques previously developed for type I optogenetic experiments.

Associated Enabling Technologies for Optogenetics in Neuroscience: Opsin Targeting

While optogenetic tools are continuously being optimized for efficient transcription, expression, and safety, a successful neuroscience experimental paradigm additionally requires specific in vivo targeting of the optogenetic tool. In this section we review generalizable in vivo delivery and targeting strategies. Major categories include (1) viral promoter targeting, (2) projection targeting, (3) transgenic animal targeting, and (4) spatiotemporal targeting—subsets of which may be combined for further increased specificity.

Targeting with Viruses

Viral expression systems have numerous advantages for optogenetics, including rapidity and flexibility of experimental implementation, potency linked to high gene copy number, and capability for multiplexing genetic and anatomical specificity as described below. Indeed, viral vectors currently represent the most popular means of delivering optogenetic tools to intact systems. For example, lentiviral vectors (LV; Dittgen et al., 2004) and adeno-associated viral vectors (AAV; Monahan and Samulski, 2000) have been widely used to introduce opsins into mouse (e.g., Adamantidis et al., 2007; Petreanu et al., 2009; Haubensak et al., 2010; Ciocchi et al., 2010; Lobo et al., 2010; Kravitz et al., 2010), rat (e.g., Aravanis et al., 2007; Gradinaru et al., 2009; Lee et al., 2010), and primate (Han et al., 2009; Busskamp et al., 2010; Diester et al., 2011) neural tissues. These vectors have achieved high expression levels over long periods of time with little or no reported adverse effects. LV may be easily produced using standard tissue culture techniques (Zhang et al., 2007, 2010), while AAV may be more challenging to produce within standard laboratory environments and can be produced either by individual laboratories (e.g., using kits such as Virapur) or through core virus production facilities (e.g., University of Pennsylvania, Stanford University, and University of North Carolina, where we have arranged a process by which useful quantities of live virus for experiments may be obtained economically from much larger preparations of commonly used optogenetic viruses). AAV-based expression vectors display low immunogenicity and offer the advantage of viral titers that result in larger transduced tissue volumes compared with LV. Additionally, AAV is considered safer than LV since currently available strains do not broadly integrate into the host genome and are rated as BSL1, compared with the BSL2+ LV. Both viruses support pseudotyping techniques that in principle enable a range of cell-type tropisms and transduction mechanisms. The high multiplicity-of-infection achieved with LV and AAV is particularly useful for optogenetics, as high copy numbers of opsin genes are required to ensure robust photocurrent responses in vivo.

Among the most widely used AAV vectors are recombinant AAV2 (rAAV2) vectors pseudotyped with various serotype packaging systems (e.g., rAAV2/2 or rAAV2/5, referred to simply as AAV2 or AAV5 here). AAV2 differs from AAV5 in the degree of viral spread, in both rodents (Paterna et al., 2004) and primates (Markakis et al., 2010). A microliter-scale volume of AAV5 injected into mouse hippocampus will diffuse and transduce neurons through much of the entire structure. In contrast, injections of AAV2 in the CNS can result in a relatively restricted expression pattern and thus may be suitable for experiments where local expression is desirable (Burger et al., 2004). LV is even more restricted in its diffusion in vivo and can be used to target subfields of a structure such as the CA1 region of the mouse hippocampus. Differences in trafficking might be related to relative distribution of binding partners in the neuropil; AAV2 is known to transduce neurons via proteoglycan molecules, using FGF receptors and integrins as coreceptors (Summerford and

Table 2. Characterized Viral Promoters for Specific Optogenetic Targeting

Vector	Promoter (serotype)	Size	Organism	Cell-Type Specificity	References
Lentivirus					
	EF1α	1.2 Kb	Rat, mouse	Neuron-specific only in LV*	Jakobsson et al., 2003
	CMV	0.6 Kb	Rat, mouse	Nonspecific (8.6% glia expressing transgene)	Blömer et al., 1997; Jakobsson et al., 2003; Dittgen et al., 2004
	Human SynapsinI (hSynI)	0.5 Kb	Rat, mouse	Panneuronal, but a tropism for excitatory cells in LV	Dittgen et al., 2004; Nathanson et al., 2009b; Diester et al., 2011
	CaMKIIα	1.3 Kb	Macaque, rat, mouse	Excitatory neurons in cortex and hippocampus	Mayford et al., 1996; Dittgen et al., 2004; Aravanis et al., 2007
	hGFAP	2.2 Kb	Rat, mouse	Astrocytes	Brenner et al., 1994; Jakobsson et al., 2003; Gradinaru et al., 2009; Gourine et al., 2010
	TPH-2	2 Kb	Rat	Raphe serotonergic neurons	Benzekhroufa et al., 2009b**
Adeno Associated Virus					
	CaMKIIα (AAV5)	1.3 Kb	Macaque, rat, mouse	Excitatory CaMKIIα neurons in cortex, amygdala.	Lee et al., 2010; Tye et al., 2011
	hSynI (AAV2)	0.5 Kb	Macaque, rat, mouse	Panneuronal, but a tropsim for inhibitory cells at low titers	Nathanson et al., 2009b; Diester et al., 2011
	hThy1 (AAV5)	5 Kb	Macaque	Panneuronal	Diester et al., 2011
	fSST (AAV1)	2.6 Kb	Macaque, rat, mouse	Inhibitory neurons (no subtype specificity)	Nathanson et al., 2009a
	hGFAP (AAV5, AAV8)	2.2 Kb	Rat	Astrocytes	Lawlor et al., 2009; Lee et al., 2010
	MBP (AAV8)	1.35 Kb	Rat	Oligodendrocytes	Lawlor et al., 2009
	SST (AAV2)	2 Kb	Rat	preBötzinger C somatostatin neurons	Tan et al., 2008

Specificity might vary with organism and brain region. Specificity needs to be evaluated for each individual construct and vector.
*Some nonspecific promoters, such as EF1α, can appear neuron specific in lentivirus but not in other vectors.
**This study also uses a novel IRES-based single-vector Gal4/p65 amplification system, which might be applicable in other weak promoters.

Samulski, 1998; Qing et al., 1999; Summerford et al., 1999), while AAV5 binds sialic acid and enters neurons through PDGF receptors (Di Pasquale et al., 2003). Additional AAV serotypes are continually undergoing characterization (Broekman et al., 2006; Lawlor et al., 2009), with a reported diversity of > 120 different AAV subtypes yet to be tested. Notably, molecular engineering is being applied to the capsid proteins of AAV to generate novel tropisms for a wider range of cell-type specificity with hybrid AAVs (Choi et al., 2005; Markakis et al., 2010), and the growing interest in the use of AAV vectors for gene therapy will undoubtedly facilitate the characterization of these new vectors and yield improved targeting strategies for optogenetics.

Crucially, with viral expression, targeting specificity can arise from multiple intersecting mechanisms. For example, specificity for a selected neuronal population can be conferred by idiosyncratic viral tropisms for different cell types (Burger et al., 2004; Nathanson et al., 2009b), as well as by cell-type-specific promoters used to drive expression of the transgene (Brenner et al., 1994; Mayford et al., 1996; Blömer et al., 1997; Jakobsson et al., 2003; Dittgen et al., 2004; Nathanson et al., 2009a). In a comparison between expression of transgenes under the same promoter with AAV2 or lentivirus, lentiviral vectors were biased to transduction of excitatory neurons whereas low-titer AAV2 vectors expressed more in inhibitory neurons in mouse somatosensory cortex (Nathanson et al., 2009b). Promoters that are not neuron specific but do drive robust expression in neurons (such as EF1α), when expressed using AAV or VSVG-pseudotyped LV, have been used for opsin expression in mammalian brains (Deisseroth et al., 2006; Zhang et al., 2006). Only a few cell-type-specific promoter fragments are small enough to be packaged with the AAV or LV viral genome along with an opsin (Table 2), while retaining useful expression specificity properties. Astrocyte-specific promoter fragments (i.e., GFAP) have been characterized (Brenner et al., 1994) that can drive specific expression of transgenes in astrocytes (excluding neurons) both with VSVG-pseudotyped LV (Jakobsson et al., 2003) and with AAV (serotypes 8 and rh43; Lawlor et al., 2009); these have now been applied for optogenetic experiments (Gradinaru et al., 2009; Gourine et al., 2010) using the low Ca^{2+} flux through the ChR channel to trigger Ca^{2+} waves and activate astroglial signaling. The human Synapsin I (Nathanson et al., 2009b; Diester et al., 2011) and human Thy1 (Diester et al.,

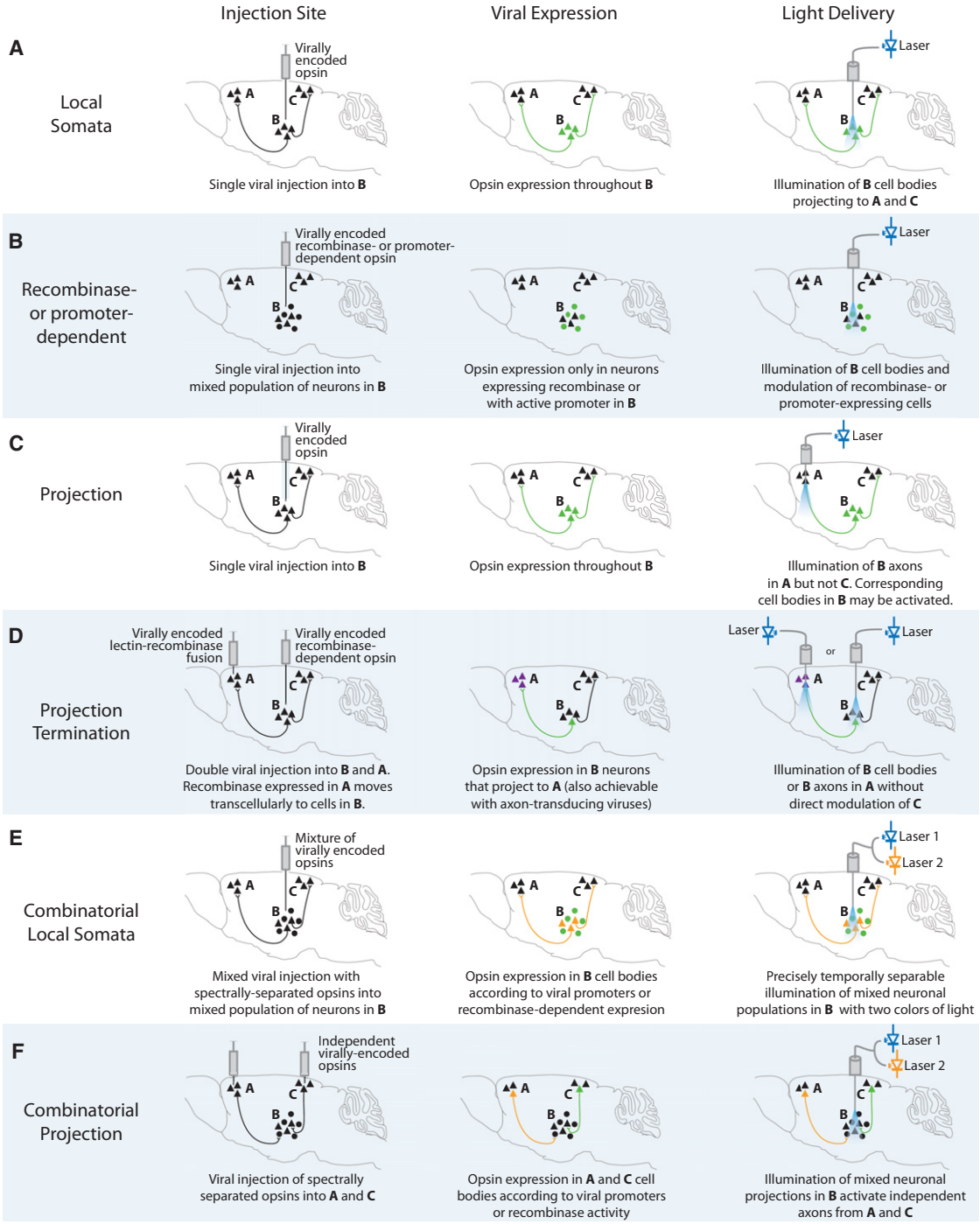

Figure 2. Targeting Optogenetic Tools In Vivo

(A) Direct stimulation of neuronal cell bodies is achieved by injecting virus at the target region and then implanting a light-delivery device above the injected region. Even this simple experiment can provide specificity with viruses that will not transduce afferent axons and fibers of passage.

(B) Additional cell-type specificity is attained either by cell-type-specific promoters in the viral vector or via a recombinase-dependent virus, injected in a transgenic animal expressing a recombinase such as Cre in specific cells, leading to specific expression of the transgene only in defined cell types.

(C) Projection (axonal) targeting is achieved by viral injection at the region harboring cell bodies, followed by implantation of a light-delivery device above the target region containing neuronal processes from the virally transduced region; in this way cell types are targeted by virtue of their projections.

(D) Projection termination labeling is a more refined version of projection targeting, in which cells are targeted by virtue of synaptic connectivity to the target region and likely excluding cells with axons simply passing through the region. Transcellular labeling using a recombinase-dependent system is shown. Viruses expressing Cre fused to a transneuronal tracer (lectin) are delivered at the synaptic target site, and a Cre-dependent virus is injected into the region with cell bodies. Cells that project to the Cre-injected area express the Cre-dependent virus and become light sensitive. This can also be achieved with axon terminal-transducing viruses although without control over the postsynaptic cell type.

2011) promoters can be used to selectively target opsins to neurons (excluding glia) in a range of systems from rodent to primate (see Table 2).

It remains a major challenge to identify neuron-type-specific promoter fragments small enough to be packaged into viral payloads, certainly in primate tissues but also in rodents and other experimental systems. Several inhibitory neuron-specific promoters have been characterized, although these are not specific to subsets of inhibitory cells (Nathanson et al., 2009a; Table 2). For broad excitatory neuron targeting, the Ca^{2+}/calmodulin-dependent kinase II alpha (CaMKIIα) promoter has been shown to express mainly in excitatory neurons in cortex and hippocampus (Dittgen et al., 2004), and for many years has been applied for optogenetic control in a range of systems (Aravanis et al., 2007; Zhang et al., 2007; Han et al., 2009; Sohal et al., 2009; Johansen et al., 2010; Lee et al., 2010). Finally, in certain systems, specific virus-compatible promoters for hypocretin neurons, serotonin neurons, and somatostatinergic neurons have been described (Adamantidis et al., 2007; Tan et al., 2008; Benzekhroufa et al., 2009a, 2009b; Tan et al., 2010; Table 2). An important caveat, however, is that promoter specificity observed in one region of organism may not hold in other tissues or organisms, and promoter and tropism strategies are not truly generalizable. Additionally, promoter specificity must be accompanied by viral access: a given neuron must both express the viral receptor and the promoter in order to be specified in this manner. Where available, each promoter must be characterized for cell-type specificity within the context of the chosen viral vector, organism, and brain region.

For simple optogenetic applications with small promoters, such as the expression of an opsin gene tagged with a fluorescent protein, AAV vectors are sufficient. However, expression of larger genes and larger promoters, or coexpression of more than one optogenetic tool, requires careful consideration when choosing the appropriate vector. The main challenge in achieving specific expression with viral targeting is that the genome size contained in a viral capsid is limited, depending on the virus type and serotype. For example, LV particles can carry a genome of up to 9 kb (Kumar et al., 2001), including the regulatory elements and viral genes encoded within. AAV-based vectors are generally restricted to a genome size of 4.7 kb, although new methods might facilitate expression of larger genomes (Dong et al., 1996, 2010). For expression of even larger genomes (e.g., with larger promoter fragments or transgenes), adenoviral vectors can carry up to 27 kb of genetic material (Soudais et al., 2004). Herpes simplex-based vectors (HSV; Lilley et al., 2001; Lima et al., 2009; Covington et al., 2010; Lobo et al., 2010) also have greater carrying capacity and offer the potential for transducing axon terminals more efficiently than LV or most AAV serotypes, although consistency and toxicity are concerns for HSV approaches (Fink et al., 1996). This axonal-transduction property (shared with rabies viruses, pseudotyped LVs, some AAVs, and pseudorabies viruses (Kaspar et al., 2002; Burger et al., 2004; Kato et al., 2007; Callaway, 2008; Miyamichi et al., 2011; Kato et al., 2011) can be either a feature or a bug in a given optogenetic experimental paradigm. This property when utilized diminishes one of the valuable specificities of virus-based optogenetics, which has been confinement of opsin gene transduction to local cell bodies without the confound of transducing (and photosensitizing) incoming afferents (e.g., Lee et al., 2010). On the positive side, such "retrograde" transduction provides one means for targeting neurons based on connectivity (although other methods described below exist to achieve this goal).

As noted above, relying on idiosyncratic known viral tropisms or finding suitable virus-borne promoter fragments is not currently available for optogenetic control of most neuronal subtypes. However, the strategy of designing viruses that can leverage the large and rapidly growing armamentarium of animal lines that express exogenous recombinases only in defined cell types (driver lines, which can fully capitalize on enormous native promoter/enhancer regions rather than the small fragments which fit into viruses) offers an expanded range of opsin targeting strategies (Figure 2B; see Table 3 for driver lines used in optogenetic studies). New driver lines are continually added to the available repertoire by groups such as GENSAT and the Allen Institute for Brain Science. Successfully utilizing a recombinase driver line requires efficient packaging of the genetic material to be expressed into a recombinase-dependent system conferring the two properties of (1) very low leak (background) of opsin expression in non-recombinase-expressing cells, and (2) very high recombinase-induced opsin expression—all within the viral backbone.

Several potential different recombinase-dependent viral vector designs have emerged (Kuhlman and Huang, 2008; Zhang, 2008; Atasoy et al., 2008; Sohal et al., 2009), and a Cre recombinase-dependent double-floxed inverted opsin gene in AAV under the EF1α promoter (Zhang, 2008; Sohal et al., 2009) or the CAG promoter (Atasoy et al., 2008) was ultimately found to provide a suitable combination of strength and specificity to enable behaviorally significant optogenetic gain or loss of function within the constraints of the freely moving mammal system (Tsai et al., 2009; Aponte et al., 2011). Not only is this strategy versatile in the sense that it can be applied at will to the large and growing pool of Cre driver lines (e.g., Gong et al., 2007), soon to include rat as well as mouse lines, but this approach is also by design expandable along new dimensions that enable combinatorial experiments (Figure 2). First, other recombinases such as Flp or Dre may be used to construct orthogonal driver lines that can be crossed with Cre driver lines while the same low-leak, high-potency recombinase-dependent AAV design is theoretically adaptable for these other recombinases as well. Second, promoter fragments may be used at the same time in place of the EF1α promoter in the recombinase-dependent viruses, thereby implementing intersecting promoter and recombinase-dependent specificity. Third, while generation of recombinase-dependent opsin mouse lines for simply crossing with Cre driver lines is a viable approach (Madisen et al., 2010a,

(E) Expression of two opsins with different characteristics in one brain region using a combination of promoter or Cre-based approaches. Light delivery to the somata is performed using two different wavelengths designed to minimize cross-activation.
(F) Projections from two different brain regions are differentially stimulated with two wavelengths matched to the respective opsins expressed upstream.

Table 3. Cre Driver Mouse Lines Successfully Employed for Biological Findings in Optogenetic Studies

Mouse Line	Expression In	Vector Used	Use References
PV::Cre	Cortical fast-spiking inhibitory interneurons	AAV-DIO-ChR2(H134R)-EYFP AAV-DIO-ChETA-EYFP AAV-DIO-eNpHR2.0-EYFP	Cardin et al., 2009; Sohal et al., 2009; Gunaydin et al., 2010
D1-Cre, D2-Cre	Striatal medium spiny neurons of the direct and indirect pathway	AAV-DIO-ChR2(H134R)-EYFP	Gong et al., 2007; Kravitz et al., 2010; Lobo et al., 2010
CaMKIIa-Cre	Excitatory neurons in cortex, hippocampus	AAV-DIO-ChR2(H134R)-mCherry	Cardin et al., 2009
Six3-Cre	Mostly cortical layer 4 neurons	AAV-FLEX-ChR2(H134R)-mCherry	Petreanu et al., 2009
ChAT-Cre	Cholinergic neurons	AAV-DIO-ChR2(H134R)-EYFP AAV-DIO-eNpHR3.0-EYFP	Witten et al., 2010; Chuhma et al., 2011
TH-Cre	Dopaminergic neurons (VTA), Noradrenergic neurons (LC)	AAV-DIO-ChR2(H134R)-EYFP AAV-DIO-eNpHR2.0-EYFP AAV-DIO-eNpHR3.0-EYFP	Tsai et al., 2009; Carter et al., 2010
DAT-Cre	Dopaminergic neurons	AAV-DIO-ChR2(H134R)-mCherry	Brown et al., 2010; Stuber et al., 2010
ePet-Cre	Serotonergic neurons (Raphe)	AAV-DIO-ChR2(H134R)-mCherry	Depuy et al., 2011
Gad2::Cre-ER^{T2}	Cortical inhibitory neurons	ROSA26::ChR2-EGFP transgenic mouse	Kätzel et al., 2011
Agrp-Cre *pomc-Cre*	Hypothalamic Agrp neurons Hypothalamic pomc neurons	AAV-FLEX-*rev*-ChR2:tdtomato	Aponte et al., 2011
PKCδ-GluCl-IRES-Cre	Amygdala *PKCδ*+ neurons	AAV-DIO-ChR2(H134R)-EYFP	Haubensak et al., 2010

2010b; Kätzel et al., 2011; Zariwala et al., 2011), resulting opsin expression levels may be weaker than with high-copy-number recombinase-dependent viruses, and more importantly the viral approach provides a unique advantage of intersecting genetic and anatomic specificity.

To illustrate this point, consider that for most Cre driver lines, specificity exists only at particular points in space and time. For example, consider a tyrosine hydroxylase (TH)::Cre line crossed with a Cre-dependent opsin mouse line; even transient expression of Cre in any cell that contained an active TH promoter at any developmental time point could serve to permanently activate opsin expression in that cell by irreversibly recombining the Cre-dependent opsin locus. While this property could be useful for developmental or cell-history information if properly controlled, and when not desired this effect can be addressed with inducible Cre driver lines (e.g., IRES-Cre-ER^{T2}; Kätzel et al., 2011), potential leak in the baseline inducibility of such systems must be considered, and a more fundamental confound also exists. In this example, the tyrosine hydroxylase (TH)::Cre drivers will express Cre not only in dopaminergic cells and fibers from the VTA and substantia nigra, but also in widely projecting noradrenergic cells from the solitary tract nucleus and locus coeruleus. This is a general problem; for example, in parvalbumin (PV)::Cre lines or other GABAergic lines, known nonlocal projections will confound the interpretation of local targeted-neuron function. In contrast, selective injection of a Cre-dependent virus in one or another of these anatomical loci at a defined moment in time in a Cre-driver organism (Tsai et al., 2009; Carter et al., 2010; Haubensak et al., 2010) provides additional specificity and enhances the utility of the opsin driver lines (Figure 2A). For example, in an elegant series of experiments, Anderson and colleagues were able to show that PKCδ+ GABAergic neurons in the CeL nucleus of the amygdala provide feed-forward inhibition onto CeM nucleus "output" neurons, using ChR2 expressed by Cre-dependent virus in a PKCδ+ mouse driver line; due to the precision of the virus approach, PKCδ+ specificity in the Cre driver line was only required in that specific circuit at that specific phase of organismal life. Optogenetically activated PKCδ+ neurons were driven while simultaneously recording from output (PAG-projecting) CeM neurons retrogradely labeled with a fluorescent tag, and it was observed that blue light produced direct GABAergic inhibition of CeM spiking (Haubensak et al., 2010).

Genetically guided optogenetic investigations now can include multiple forms of transgenesis and optical control (e.g., Kravitz et al., 2010; Lobo et al., 2010; Higley and Sabatini, 2010). However, the concept of a "cell type" may not always be definable genetically. While a simple form of the genetic identity concept could encompass a wide swath of possible cell types spanning major aspects of neurotransmitter/neuromodulator function, receptor expression, biophysical properties governed by ion channel expression, developmental origin, and the like, it is also possible that cells could look the same from the genetic standpoint but serve fundamentally different functions by virtue of differential wiring. This important concept happens to dovetail well with a unique and surprising strength of optogenetics termed "projection targeting"; this is the ability to selectively drive or inhibit cells defined by their wiring or projections.

Projection Targeting

Microbial opsin gene products, especially with assistance from molecular engineering such as the addition of cellular trafficking

motifs (e.g., Gradinaru et al., 2008, 2010), may traffic down dendrites (Lewis et al., 2009; Gradinaru et al., 2010; Greenberg et al., 2011) or axons (Gradinaru et al., 2010; Lewis et al., 2011) and create light-sensitive projections. This property, in the setting of anatomical specificity provided by viruses, allows transduction of cell bodies in one brain region and illumination of axonal projections in another (Gradinaru et al., 2007, 2009; Petreanu et al., 2007; Lee et al., 2010; Tye et al., 2011; Figure 2C), thereby defining a cell population for excitation or inhibition by virtue of its connectivity. The effects provided by a channelrhodopsin when present in an axon terminal may act via the combined influence of voltage-gated Na^+ channels and voltage-gated Ca^{2+} channels (perhaps along with, and under certain conditions, the direct but small Ca^{2+} conductance of channelrhodopsins; Zhang and Oertner, 2007), with resulting release of neurotransmitters and activation of downstream neurons. Stimulation of presynaptic terminals with optogenetic tools has been reported to lead to a remarkably high probability of release (p_r) in hippocampal CA3-CA1 synapses, associated with paired-pulse depression, in contrast with a lower p_r and paired-pulse facilitation resulting from electrical stimulation (Zhang and Oertner, 2007). Several studies have taken advantage of these properties to elucidate the synaptic output of defined axonal projections into brain regions, both in the slice preparation (Petreanu et al., 2007; Gradinaru et al., 2007; Zhang and Oertner, 2007; Cruikshank et al., 2010; Stuber et al., 2010) and in vivo (Gradinaru et al., 2009; Hull et al., 2009; Lee et al., 2010; Tye et al., 2011). This approach could ultimately be extended to the use of two excitatory opsins expressed in two brain regions, the afferents of which converge onto a third region. Optical stimulation with the appropriate wavelengths in principle could then be used to combinatorially drive synaptic activity in the two pathways (Figure 2F).

A major caveat of this approach is that "projection targeting" of a cell means only that a cell is being targeted by virtue of its projection; while this alone is very useful, without further validation it may not be assumed that only a specific projection of a cell is being excited or inhibited in isolation, due to the possibility of antidromic propagation of evoked spikes, and even antidromic spread of hyperpolarization. Where important for experimental interpretation, such possibilities must be carefully considered with control measurements (e.g., Tye et al., 2011). In some settings, it may be found that it is an entire cell (defined by possessing the illuminated projection) that is being recruited, and in many cases this will be precisely what is desired. In other cases, it may be found that only the projection is being controlled with little or no effect at the soma; again in other cases this will be the desired effect. Regardless, where important this parameter should be explored in the system under investigation, as the net effect may depend upon axon caliber, myelination status, length, and branching properties, as well as upon illumination conditions and opsin gene properties (discussed in Tye et al., 2011).

This approach provides a versatile promoter-independent means to control cells, requiring only anatomical information, and even with simple light guidance strategies this method can be applied to projections as short as hundreds of micrometers (Tye et al., 2011). A caveat of this approach is that all local photosensitive axons will be driven by light, even fibers of passage that do not synapse in the illuminated region. Controls to define a projection termination can be conducted by pharmacologically inhibiting synaptic receptors in the target region, but even more refined "projection termination targeting" strategies are possible, involving labeling of cells for optogenetic control based on formation of synapses in a defined anatomical location. For example, a transsynaptic or transcellular tracer protein such as wheat germ agglutinin (WGA) fused to Cre recombinase can be expressed in cells of interest in the synaptic target location (Gradinaru et al., 2010), while in the candidate projection-source region a Cre-dependent opsin virus may be injected (Figure 2D). In this configuration, with appropriate experimental conditions, only neurons that form synaptic terminations in the target region will receive Cre directly and express the opsin. A major caveat is that this approach may not function in the same way in all circuits, and the properties of the transcellular transport must be validated in each experimental system, as anterograde and retrograde trafficking are both theoretically possible (discussed in Gradinaru et al., 2010), and in principle at longer timescales multiple synapses could be traversed. One advantage of this overall approach—if appropriate controls are conducted and successful transcellular transport observed—is that light may in this case be delivered at the cell body (a configuration that can be especially robust), while retaining specificity of the manipulation to those cells that make the desired projection (Figure 2D).

A similar approach may be applied using axon terminal-infecting or retrogradely transported viruses such as rabies or herpes simplex virus (Callaway, 2008) or the canine adenovirus (CAV; Hnasko et al., 2006), although some concern exists over possible toxicity, especially when membrane proteins are expressed using these viral systems. Interestingly, some AAV serotypes (generally better tolerated) are also modestly capable of axon terminal infection or retrograde transport (Burger et al., 2004; Towne et al., 2010). Recently, a modified retrograde approach has been developed to map the entire synaptic network converging onto a single cell, labeled with in vivo microelectroporation (Marshel et al., 2010), a technical advance that could well dovetail with optogenetic control.

Transgenic Animal Targeting

As described above, the limitations imposed by packaging capacity in viral systems can be overcome using single-component optogenetic tools (for example, by using recombinase-dependent opsin-expressing viruses and/or by leveraging relevant anatomy for projection targeting). Beyond the benefits of speed, flexibility, spatiotemporal targeting precision, and high gene copy-number, virus injection into recombinase driver lines also can uncouple promoter specificity from expression strength, since opsin expression is related to the copy number of the virus with its strong nonspecific promoter, and resulting transcription can exceed endogenous transcription from tissue-specific promoters. However, another major class of strategy, generation of mouse transgenic lines directly expressing opsin genes under local promoter-enhancer regions (i.e., not in a recombinase-dependent fashion), provides a distinctly useful means of achieving cell-type-specific opsin expression. While transgenic mouse lines require effort, time,

and cost associated with production and maintenance, the convenience and reliability of homogeneous opsin-expressing animals provides major experimental leverage.

The Thy1::ChR2-EYFP mouse lines (Arenkiel et al., 2007; Wang et al., 2007) express ChR2 under control of the Thy1 promoter. While as discussed above promoters do not suffice to completely define cell types and the complement of labeled cells must be considered in each case, Thy1-driven expression is largely restricted to projection neurons, enabling several studies in which optogenetics was applied to study cortical connectivity (Wang et al., 2007), transmission from the olfactory bulb to cortex (Arenkiel et al., 2007), aspects of ganglion cell function in visual impairment (Thyagarajan et al., 2010), cortical information processing (Sohal et al., 2009), and parkinsonian circuitry (Gradinaru et al., 2009). For example, in the latter study it was found that therapeutic deep brain stimulation (DBS) in the subthalamic nucleus (STN) arising from a point source (e.g., electrode or fiber) is by far most effective when the direct target is afferent axons within the structure (these axons then efficiently modulate both downstream and upstream neurons—and indeed potently reduce local STN spiking); much weaker effects were seen with direct modulation of local cell bodies in the STN by a point source of control, suggesting electrical DBS might be best designed to target axonal tracts rather than gray matter.

A defined local cell type was targeted in a pioneering study by Kiehn and colleagues (Hägglund et al., 2010), in which VGLUT2 cells in the spinal cord expressed a channelrhodopsin. Optically controlled activation of specific groups of excitatory neurons in either the mouse spinal cord or hindbrain was found to evoke stereotypical locomotion, illustrating the principle of precise optogenetic control of transgenically defined neurons in the context of a well-defined, complex, and behaviorally significant behavioral output (Hägglund et al., 2010). This approach is generalizable as well, and many additional transgenic opsin-expressing mouse lines have now been described (Zhao et al., 2010; Ren et al., 2011) as well as conditional opsin lines discussed in more detail below (Kätzel et al., 2011; Chuhma et al., 2011); for example, the latter study utilized a tTA/tetO strategy and crossed two mouse lines to achieve specific expression of a channelrhodopsin in striatal medium spiny neurons (Chuhma et al., 2011).

Spatiotemporal Targeting

Cells may also be targeted by virtue of their birthdate or proliferation status, location at a moment in time, and other versions of what might be called "spatiotemporal" targeting; this approach has reached its most advanced state in the course of targeting specific neocortical layers (Petreanu et al., 2007, 2009; Gradinaru et al., 2007; Adesnik and Scanziani, 2010).

A long-sought goal of neuroscience has been to tease apart the role of specific layers, and of layer-specific neurons, in cortical microcircuit processing, brain-wide network dynamics, and animal behavior. In utero electroporation (IUE) may be employed to target opsins to distinct layers of the cortex, capitalizing on the sequential layer-by-layer ontogeny of neocortex in mammals, by incorporating the DNA into neurons generated during a specific embryonic stage (Petreanu et al., 2007, 2009; Huber et al., 2008; Adesnik and Scanziani, 2010). Beyond this special targeting capability, an additional unique advantage of IUE is that opsins are expressed from before the time of litter birth (allowing electrophysiological experiments at a younger stage than with viral expression).

Optogenetic tools have been well tolerated when electroporated into mouse embryos in naked plasmid form. In principle, cells may also be targeted for optogenetic control by (1) active proliferation status at a particular moment in time, using cell-cycle-dependent Moloney-type retroviruses (Toni et al., 2008); (2) location at a particular moment in time (e.g., via migration through a particular anatomical location during development; and (3) other methods including ex vivo sorting followed by transduction and transplantation. In general, the range of genetic techniques for delivering opsin genes into the brain has become broad and versatile and leverages the intrinsic tractability of the single-component microbial opsin tools.

Associated Enabling Technologies for Optogenetics in Neuroscience: Light Delivery

Once the desired opsins have been targeted to neurons of interest, the next experimental consideration is light delivery. Requirements vary widely across experimental paradigms. For instance, a multiple-opsin study of fast oscillations in a brain slice preparation will require a different light delivery approach than a study of the effects of prolonged stimulation of a deep brain nucleus in a behaving animal. Next we review strategies for meeting the light requirements for particular experimental applications via the spatial, temporal, and spectral control of illumination.

Light Requirements for Activation at the Molecular and Cellular Level

The photocurrent in a neuron resulting from a pulse of light will depend upon many factors, including the properties of the opsin being expressed, the wavelength, intensity and duration of the incident light, and even recent illumination history (if fewer channelrhodopsin molecules begin in or have returned to the dark-adapted state, the initial transient response to a light pulse will be smaller, though the steady-state photocurrent may remain the same; Boyden et al., 2005; Rickgauer and Tank, 2009). In all cases, however, the rate of absorption of photons of a given wavelength is proportional to the local photon flux; that is, the number of photons incident per unit time per unit area. When designing a light delivery system to activate rhodopsins, it is therefore chiefly this parameter that we wish to measure and control.

Given the ease of measuring total light power (in Watts) using commercially available light power meters, it is more convenient to measure and report "light power density" (typically measured in mW/mm^2), rather than photon flux. Light power density is simply the photon flux multiplied by the energy of the individual photon, which is inversely proportional to wavelength. For wild-type ChR2 at typical expression levels and illuminated with 473 nm light, light power densities of ~1–5 mW/mm^2 were initially found to be sufficient to elicit action potentials (Boyden et al., 2005). Light requirements vary among different optogenetic tools, and one must consider the specific properties of the opsin-retinal complex when designing the experiment. For example, optogenetic inhibition may require continuous light for as long as inhibition is desired, whereas bistable optogenetic

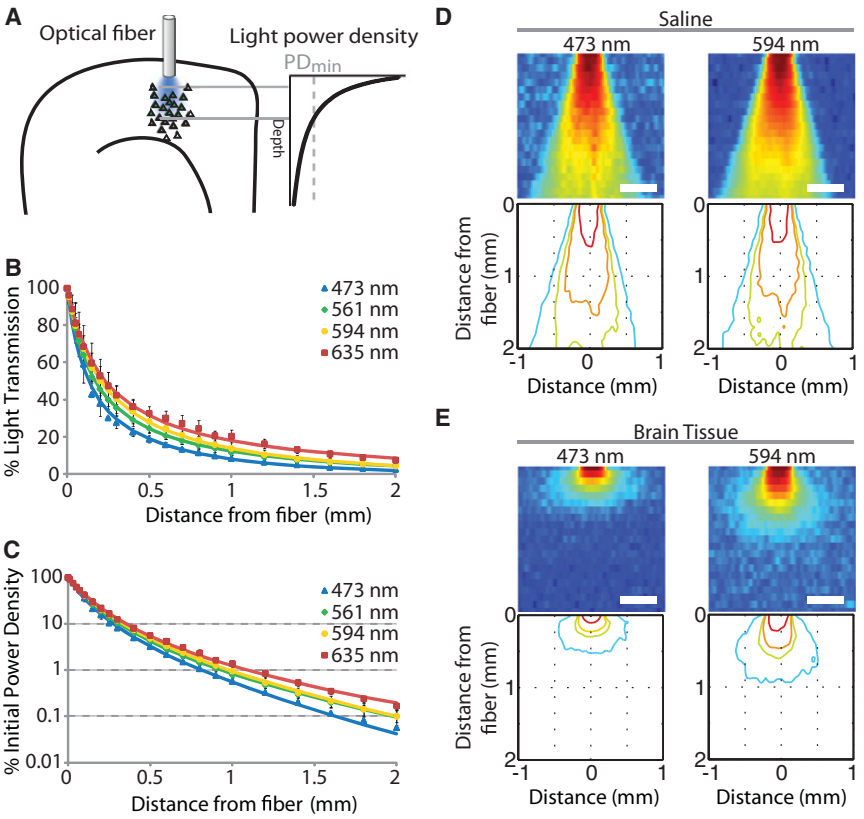

Figure 3. Light Propagation in Brain Tissue for In Vivo Optogenetics

(A) Schematic showing that the maximum activation depth is the depth at which the light power density falls below the activation threshold, PD_{min}.

(B) Measured percent transmission of light power at 473 nm, 561 nm, 594 nm, and 635 nm light from a fiberoptic (200 μm, NA = 0.37) shown as a function of distance from the fiber tip in brain tissue. Solid lines represent fits to the measured data (Aravanis et al., 2007).

(C) Predicted fraction of initial light power density as a function of depth in brain tissue for the same fiber; includes effects of absorption, scattering, and geometric light spread.

(D and E) Lateral light spread as a function of sample thickness. Saline solution (top) or rat gray matter (bottom) was illuminated by either blue (473 nm; left) or yellow (594 nm; right) light delivered through a 200 μm optical fiber (NA = 0.37). Images are sections through a 3D map of light intensity along the axis of an illuminating fiber. Contour maps of the image data show iso-intensity lines at 50%, 10%, 5%, and 1% of maximum. Note conical spread of light in saline due to fiber properties, and more symmetrical light propagation shape in brain tissue.

control (Berndt et al., 2009) only requires brief, widely spaced light pulses, typically at much lower power (<0.01 mW/mm^2).

We recommend that the light power density, rather than total power, be reported in optogenetic studies. When illuminating cultured cells with light coupled into a microscope's beam path, calculating light power density can be as simple as dividing the total emitted light power by the area of the illuminated spot. However, when shaped beams of light are directed into larger volumes of tissue, such as with optical fiber illumination of the intact brain, estimating light power density at the targeted location requires accounting for attenuation introduced by beam divergence and the optical properties of the illuminated tissue (Aravanis et al., 2007 and see below). Such calculations also help estimate the volume of tissue recruited by the light stimulus in vivo and are critical for the design and interpretation of experiments.

Optical Properties of Brain Tissue

For a given opsin gene, functional expression levels and the light power density reaching the expressing cells will together determine the efficacy of light-based control (Figure 3A). To estimate this density of light reaching the targeted cells one must consider the propagation of light in tissue. Light propagation in biological tissue can be modeled as a combination of absorption and scattering, with scattering playing an especially important role in mature myelinated brain tissue (Vo-Dinh, 2003). The transmission properties of light through the brain also depend strongly on wavelength, with longer-wavelength light scattering less and therefore penetrating more deeply (Figure 3).

We have taken several complementary approaches to measuring and estimating the depth of light propagation under typical experimental conditions, specifically for the illumination of deep brain structures using thin optical fibers. In one approach (Aravanis et al., 2007), an optical fiber emitting a known light power was lowered into a block of unfixed brain tissue, and light power was measured on the underside of the block, giving a transmission fraction for the tissue sample (nontransmitted light was either absorbed by or reflected out of the sample). This measurement was repeated for a range of tissue thicknesses by stepping the fiber through the block. These data were fit with standard equations for the propagation of light in diffuse scattering media (Kubelka-Munk model; Vo-Dinh, 2003), in order to estimate parameters that could be used to predict depth of transmitted light power in other experimental configurations.

To estimate the light power density at a given distance from the fiber tip, the beam was modeled as spreading conically within the tissue, with an angle determined by the optical properties of the fiber. This model, while involving a number of unrealistic assumptions including that the sample is a homogeneous, ideal diffuser illuminated from one side with diffuse light, and that reflection and absorption are constant over the thickness of the sample, nevertheless allowed a good fit to measured data (Figures 3B and 3C; Aravanis et al., 2007) when used to estimate light power density at progressively deeper sites. Next, to directly observe the lateral spatial extent of the illuminated region at various distances from the fiber, we repeated the experiments above with the block of brain tissue placed on a thin diffusing layer revealing the two-dimensional pattern of illumination at the bottom of the block; this screen was imaged from below as the fiber was lowered through either brain tissue, or saline

solution, and the resulting images were stacked to create a three-dimensional volume (Figures 3D and 3E). The light power density profiles directly below the fiber were in general agreement with the attenuation predicted by the simple conical model, for distances corresponding to relative light power densities down to 5% of the initial value. At greater distances, the higher number of scattering events results in a higher degree of lateral spread. A useful rule of thumb based on these direct measurements (Figure 3E) is that the full (edge to edge) width of lateral light spread, arising from an optical fiber in gray matter, is quantitatively similar to the full depth (fiber tip to edge) of forward light spread at a given light level.

These direct measurements provide the basis for a quantitative estimation of the volume of tissue recruited during optogenetic experiments, have been validated by light measurements and electrophysiology at known distances from the illumination source (Aravanis et al., 2007; Adamantidis et al., 2007; Gradinaru et al., 2009; Cardin et al., 2009; Tye et al., 2011), and are generally consistent with immunohistochemical staining for molecular markers of elevated activity such as c-*fos* (Gradinaru et al., 2009). Complementing these measurements, estimates of transmission of light can be simulated with Monte-Carlo methods (e.g., Bernstein et al., 2008), and as the geometry and chemical composition of brain tissue are complex neither the simple models nor the Monte Carlo simulations can be relied upon without validation using direct measurements. Transmission measurements and estimated light power densities for blue (473 nm) and green (561 nm) light emitted from a fiberoptic have been previously reported (Aravanis et al., 2007; Adamantidis et al., 2007), but the advent of the new red-shifted optogenetic tools described above requires consideration of additional wavelengths of light; here, we report these values for 473 nm, 561 nm, 594 nm, and 635 nm light in brain tissue (Figures 3B and 3C). A simple calculator that estimates light power density as a function of depth in tissue, using the data reported here and allowing user input on wavelength, light power, and fiber type, is available online at www.optogenetics.org/calc. This depth estimation, when combined with the empirical observation that the full (edge to edge) width of lateral light spread is quantitatively similar to the depth of forward light spread from the fiber tip for a given contour, allows rapid estimation of illumination profiles for in vivo work. Spatial light targeting can be multiplexed with the opsin targeting strategies described above to further restrict which components of the neural circuit are modulated.

Controls for Nonspecific Effects of Opsin Expression and Light Delivery

The expression of exogenous opsins in tissue and the delivery of the light needed to activate them may also result in unintended effects, such as toxicity or tissue heating. Viral infection and the expression of exogenous proteins at high levels could alter cellular capacitance (Zimmermann et al., 2008), alter cellular physiology, or even lead to toxicity; we and others have found that the CMV, CAG, and rabies-based promoters may express opsins at very high levels that can cause protein accumulations or structural abnormalities in the targeted neurons over time. However, very long-term expression of any membrane (or other exogenous) protein with even more moderate-strength promoters can cause toxicity, and we have found that expression strength and time of expression interact in giving rise to this phenomenon. When employed, fusion proteins could appear to mimic such an effect, but some fluorescent proteins such as mCherry to which opsins are commonly fused themselves can clump and accumulate, while not necessarily impairing opsin function or cell health (e.g., Adamantidis et al., 2007). Regardless, it is important to track membrane resistance and resting potential; modest trends of effects on these membrane properties are occasionally seen with high level opsin expression. Especially when such an effect is observed, it is important to carry out no-light controls in opsin-expressing tissue or animals.

Indeed, in theory not only intrinsic neuronal properties (such as input resistance, membrane capacitance, and excitability) could be altered by toxicity linked to long-term or very high-level membrane protein overexpression, but even functional output and effective synaptic connectivity could be altered. A no-light control condition in which the tissue is virally transduced, but no light is delivered, can address these effects and is especially valuable when the light delivery paradigm does not involve switching on-and-off and therefore within-animal controls are less feasible (Tsai et al., 2009). For invertebrates such as *C. elegans* and *D. melanogaster*, where retinal is not present but may be easily supplied in food or substrate, another type of control is possible, the retinal-negative condition (Zhang et al., 2007).

Light used to activate opsins may also produce nonspecific effects. Light leaking from the delivery apparatus, or scattered through brain tissue may reach light-sensing organs such as the retina, directly affecting neural activity, or leading to changes in an animal's behavior. Light absorbed by tissue could also result in photodamage or local temperature increases. It is therefore critical that parallel no-opsin control experiments using identical illumination conditions are included in optogenetic experiments (e.g., Adamantidis et al., 2007; Tsai et al., 2009; Lee et al., 2010).

The issue of tissue heating by light deserves special consideration, since even temperature changes too small to cause detectable tissue damage can lead to significant physiological (Moser et al., 1993) and behavioral (Long and Fee, 2008) effects. Consider pulsed laser light delivered to a deep brain region by a thin optical fiber. Light is emitted in a conical pattern, then scattered and absorbed as it passes through optically inhomogeneous brain tissue. Heat will be generated wherever light is absorbed, in proportion to the light intensity at each point, giving rise to a heat source that is distributed throughout the tissue. The temperature gradient resulting from this heating will be counteracted over time by conduction of heat, by mass transfer (e.g., the perfusion of the region by blood), and possibly also by changes in metabolic heating as a result of stimulation or inhibition. Notably, both scattering and absorbance vary with light wavelength, with absorbance ~10 times higher at 475 nm than 600 nm (Yaroslavsky et al., 2002). Therefore, even under conditions of equivalent total light power delivery to the brain through the same optical fiber, the spatial structure of the resulting heat source can be markedly different for different wavelengths.

As an exercise it may be useful to estimate an upper bound for temperature changes resulting at a targeted region under

typical experimental conditions. These calculations show that expected temperature changes should always be considered but need not be in a range that might be expected to influence neurophysiology. For an optical fiber (200 μm, NA = 0.37) placed 0.5 mm above a targeted region, emitting 5 mW of blue (473 nm) light, the predicted (see above) local irradiance at the target is 4.9 mW/mm^2 (Aravanis et al., 2007). Multiplying this by the coefficient of absorption for brain tissue at 473 nm of approximately 0.1 mm^{-1} (Yaroslavsky et al., 2002), gives a local light power deposition rate of 0.49 mW/mm^3. If light is delivered to the brain as 5 ms pulses at 20 Hz for 30 s (the equivalent of 3 s of constant illumination), total energy deposition would be 0.49 × 3 = 1.47 mJ/mm^3. If we conservatively assume that this power were delivered as an impulse (i.e., ignoring the mitigating effects over time of conduction and blood flow), then given a specific heat of brain of 3650 mJ × g^{-1} × $°C^{-1}$ and a brain density of 0.00104 g/mm^3 (Elwassif et al., 2006), we would expect a local change in temperature of 1.47 / (0.00104 × 3650) = 0.38°C. Larger temperature excursions would be expected at nontargeted regions closer to the fiber tip, where irradiances are much higher. However, at such locations, the assumption of zero conduction used in the above calculation is less reasonable since the local temperature gradients would also be much steeper (due to both the exponential falloff of irradiance with distance and the proximity of nonilluminated tissue). Moreover, the light is certainly not condensed into a single impulse in optogenetic experiments, where pulsed light or delivery over time is the norm.

Deep brain temperatures in rodents are known to vary naturally over a range of several degrees C as a result of circadian rhythm, exercise, and environmental temperature (Moser et al., 1993; DeBow and Colbourne, 2003). While the expected heating from light under typical conditions is much less than this normal range, even small systematic differences between light on and off conditions could contribute to any observed behavioral or physiological effects; moreover, if investigators use higher light powers or contribute to additional heat sources with local LEDs instead of remote diodes, heating effects will become relevant. We therefore re-emphasize the need for opsin-negative controls especially in cases where continuous light is delivered, and suggest the importance of more sophisticated modeling of brain heating (such as have been developed to study thermal effects of electrical stimulation (Elwassif et al., 2006) in future work.

Light Sources

Depending on the application, some optogenetic experiments may require a light source with stringent requirements to emit a specific distribution of wavelengths with fast temporal modulation, at high power, and with a particular spatial pattern. Since microbial opsin-derived tools can be deactivated by light of wavelengths near the activation wavelength (Berndt et al., 2009), light sources with sharp spectral tuning are generally preferred over broadband light sources; sharp tuning is also critical when attempting to selectively activate a single tool in a multiple-opsin experiment. Moreover, some experiments may require precise temporal control of light power (e.g., dynamic clamp experiments; Sohal et al., 2009), while others may require especially stable continuous illumination over long periods (e.g., during a long-lasting inhibition protocol (Carter et al., 2010). And finally, achieving sufficient light output from miniaturized optical components represents another significant challenge. Here we will discuss these crucial issues in the context of light source hardware and review the benefits and limitations of various technologies currently in use.

Lasers

Lasers are an appealing option for many types of optogenetic experimentation, with a very narrow spectral linewidth (typically < 1 nm), which can be matched closely to the peak activation wavelength of the optogenetic tool of interest; moreover, many lasers can be directly modulated at kilohertz frequencies. Laser beams have a very low divergence, and so can be readily steered through various optical elements on an optical table, such as electronic shutters, beam splitters, power meters, and dichroic mirrors for combining multiple laser lines (Figure 4A). The narrow width and low divergence of laser beams are especially important when attempting to couple light into optical fibers, which require light to be focused to a small spot size (50–400 μm) at a shallow angle in order to be effectively coupled.

For integration into physiological experiments, we have found that that diode lasers and diode-pumped solid-state (DPSS) lasers are the most appropriate (Aravanis et al., 2007; Adamantidis et al., 2007). Lab-quality models are offered by several vendors (Cobolt, Omicron, Newport, Crystalaser, OEM Laser Systems) in a number of useful wavelengths across the opsin action spectrum with sufficient continuous-wave (CW) output power; these include appropriate focusing optics and mounting hardware and are compact, portable, and robust for daily lab use. We have found that direct diode lasers tend to be more reliably modulated at high speeds than DPSS lasers at similar wavelengths. Lasers with a power output of ~100 mW are typically used, driven with a power supply that allows for analog modulation of output power. This level is sufficient to generate high light power densities out of small optical fibers even after coupling and transmission losses, after splitting into multiple fibers, and after some degradation of output power with use.

Different wavelength outputs from DPSS lasers are achieved by using different combinations of pump diodes and solid-state gain media. Due to differences in the complexity, efficiency, and tolerances of these devices, and in the control electronics they require, DPSS lasers of the same power but different wavelength can vary more than 10-fold in price and have very different performance characteristics, especially with respect to temporal modulation. For instance, 473 nm and 532 nm DPSS lasers can reliably generate 1 ms pulses (though for pulses < 100 ms in duration, the average power during a pulse may be significantly less than the steady-state output at the same command voltage; Figure 4B). On the other hand, 593.5 nm (yellow) DPSS lasers cannot be reliably modulated even at the second timescale, so we employ instead a high-speed shutter in the beam path (Uniblitz, Stanford Research Systems, Thorlabs; Figure 4A). High-speed beam shutters can be acoustically noisy (though low-vibration shutters are manufactured by Stanford Research Systems), and so experiments must be designed such that this auditory stimulus time-locked to laser illumination does not become confounding for intact animal preparations (even in anesthetized preparations).

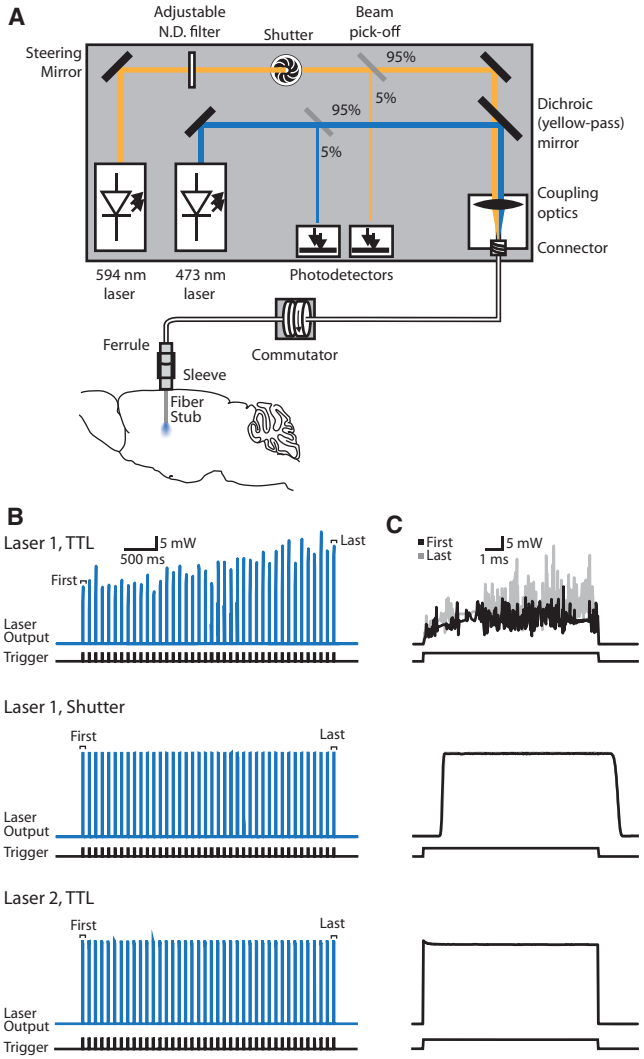

Figure 4. Two-Laser Setup for Optogenetic Stimulation

(A) Two solid-state lasers are coupled into a single fiberoptic cable for two-color modulation. A fast laser shutter is used to control the output of the yellow (593.5 nm) laser, due to its slow analog modulation. Beam pick-offs allow for online monitoring of laser output by photodetectors. An optical fiber commutator enables animals to freely move in the behavior apparatus without fiber twisting or breakage. A fiberoptic cable connects from the commutator to a fiberoptic implant consisting of a metal ferrule with a permanently attached fiberoptic cable that extends into the target region.

(B) Light power traces from three laser configurations generating 10 ms light pulses at 10 Hz for 4 s. Top: A blue (473 nm) DPSS laser (e.g., OEM lasers) directly modulated using the laser's TTL modulation mode. The upward power drift across the pulse train was repeatable. Middle: The same laser, with same command power, but in continuous operation, with modulation provided by a mechanical shutter (LS-2, Uniblitz) in the laser path. Bottom: A 488 nm direct diode laser (Phoxx, Omicron-Laserage).

(C) Expanded view of the first and last pulses from (B). Note the ramping up of power and the reduced mean power output of the DPSS laser in response to a short pulse (top) as compared to the same laser's steady state output (middle), and the ~1 ms delay introduced by the shutter (middle).

It is important to validate new equipment and all illumination protocols using a high-speed photodetector (many commercial power meters have an analog output that allows the raw light power signal to be observed on an oscilloscope). Online measurement of light power during experiments may also be achieved by using a beam pickoff that directs a small fraction of the modulated laser power to a photodetector continuously during an experiment (Figure 4A).

LEDs

Light-emitting diodes (LEDs) are another attractive light source for certain optogenetic applications. LEDs have the required narrow spectral tuning (spectral linewidth at half maximum typically in the 10 s of nm), are readily modulated at the frequencies required, are simple and inexpensive, and do not require complex control electronics; however, when used near tissue, substantial heat is generated and caution is indicated for in vivo use. Like lasers, only a limited number of colors are available that emit adequate power, though increasing the power output and spectral diversity of LEDs is an active area of research. In vitro, LEDs can serve as the light source for optogenetic experiments (Ishizuka et al., 2006; Gradinaru et al., 2007; Petreanu et al., 2007; Campagnola et al., 2008; Adesnik and Scanziani, 2010; Grossman et al., 2010; Wen et al., 2010), and LED arrays are available that permit focal stimulation of single cells, or even single neurites (Grossman et al., 2010). For in vivo applications, LEDs can be used to fill an optical fiber which is tethered to a behaving animal, but such applications are limited by the highly divergent beam pattern from LEDs with coupling efficiencies of ~1%; still, with high-power LEDs, this fraction of total power is sufficient to attain the required power density output (Gradinaru et al., 2007; Petreanu et al., 2007). Possible uses of LEDs include both direct implantation of small LEDs in or on tissue (with heating concerns requiring careful control as noted above), or permanently mounted to optical fiber waveguides carried on the subject (Iwai et al., 2011).

Incandescent Sources

Traditional broadband incandescent microscopy light sources, such as arc lamp-based epifluorescence illuminators, can be used in optogenetic experiments with appropriate narrowband spectral filters and the introduction of a shutter to the illumination beam path. Dedicated light sources with built-in high-speed shutters and filter selection are also available (e.g., the Sutter Instruments DG-4; Boyden et al., 2005) and offer pulse durations of as little as 1 ms with pulse repetition rates of up to 500 Hz. Unlike some lasers and LEDs, which offer graded modulation of intensity, shutter-based systems are limited to on/off gating of light pulses; neutral density filters can be used to produce stepped illumination. One significant advantage of the use of filtered broadband light over LEDs or lasers is the ability to select arbitrary illumination wavelengths and spectral linewidth using bandpass filters. Even more flexible are monochromators, which output commanded wavelengths via positioning of a diffraction grating.

Light Delivery: Surface Targets

In light-accessible experimental preparations such as cultured neurons, brain slices, cortical surface, or nematodes, light is typically delivered through a microscope illumination path, passing through the objective and illuminating a spot within the field of view. Apertures in the illumination path can be used to restrict this spot to a smaller portion of the field. In order to measure the light power density achieved by a given setup, a power meter can be placed below the objective; the total

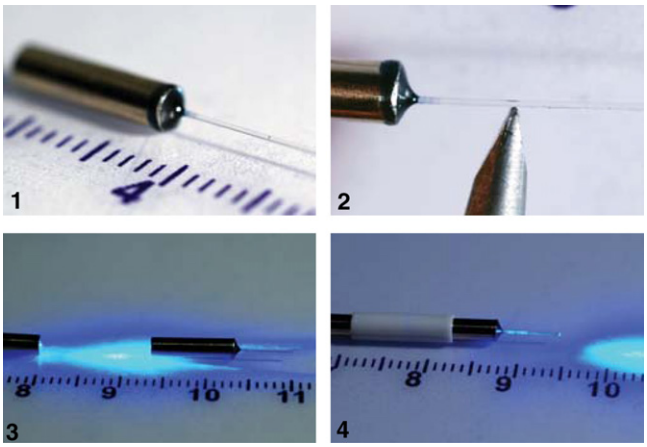

Figure 5. Implanted Fiberoptic Lightguide (IFL)
The lightguide is composed of a fiberoptic cable terminated by a metal ferrule (1). The optic fiber can be cleaved to length based on stereotactic coordinates (2) and light can then be delivered by attaching a matched fiber-ferrule pair connected to the output of the laser apparatus (3). Coupling of the fibers leads to light propagation through the implant (4).

power is measured and divided by the area of the illumination spot (Aravanis et al., 2007). For experiments requiring illumination at multiple sites, or at sites away from the imaged area, an optical fiber-coupled light source (see below) can be mounted on a micromanipulator and used to illuminate the tissue, with light power density similarly calculated from total power and spot size. Laser beams can be coupled into the microscope light path and optically expanded to fill the field of view, and moving optical elements—such as galvanometer-driven mirrors (Rickgauer and Tank, 2009; Losonczy et al., 2010), digital micromirrors (Farah et al., 2007; Arrenberg et al., 2010), or diffractive optical elements (Watson et al., 2009)—can be combined with microscope optics to deliver patterns of light to areas within the imaging field.

Indeed, spatiotemporal light patterning is a field of increasing relevance to many aspects of optogenetics (Shoham, 2010). Various methods of spatial and temporal beam shaping have been explored for delivering complex two- or three-dimensional patterns of light for single-photon (Farah et al., 2007) or two-photon control of microbial opsin-derived tools (Rickgauer and Tank, 2009; Andrasfalvy et al., 2010; Papagiakoumou et al., 2010). It remains to be seen which will be the most useful or practical method for controlling multiple cells in versatile and rapid fashion within intact tissue, but already individual cells can be controlled independently within living brain slices (Papagiakoumou et al., 2010) and freely moving worms (Leifer et al., 2011; Stirman et al., 2011), opening up immense opportunities for systems neuroscience.

Light Delivery: Deep Targets

Delivering light to in vivo preparations presents several distinct challenges compared with in vitro preparations. Light may need to be targeted to deep brain structures while minimizing damage to surrounding tissue, and in the case of behaving animals without significantly disrupting the behavior under study. To satisfy these requirements, we developed the optical neural interface discussed above for use in vivo that employs a thin optical fiber to carry light from a source (typically a laser) directly to the targeted structure (Adamantidis et al., 2007; Aravanis et al., 2007). While above we discussed the propagation of light after emerging from the fiber, here we address the fibers themselves.

Fiberoptics are thin, flexible cables made of transparent material that act as waveguides for light. The dimensions and optical properties of a particular fiber will interact with other elements in the light delivery system to affect the geometry and intensity profile of the light beam delivered to the brain. In conjunction with an understanding of the optical properties of brain tissue addressed above, such variation can be exploited in the targeting of light to particular regions (Adamantidis et al., 2007; Aravanis et al., 2007). The light-carrying fiber either can be inserted directly into the brain using a stereotaxic apparatus (for anesthetized preparations) or can be inserted into a cannula previously implanted stereotactically. Alternatively, a short length of optical fiber with one end located at the targeted brain region, and the other end terminated by a miniature fiberoptic connector (Doric Lenses, Quebec, Canada), can be permanently implanted and attached to the skull. This last method (implanted fiberoptic lightguide or IFL; Figure 5) is preferred for chronic experiments for a number of reasons; the bare fiber causes less damage than the larger cannula, the brain is completely closed to the outside environment, and mating the connector is easier and potentially less disruptive than inserting a fiber into a cannula.

The most common type of fiber, called step-index, consists of a light-carrying ''core'' material (often silica glass) surrounded by a thin ''cladding'' layer of material with a slightly higher refractive index (often a hard transparent polymer). For light delivery, fiber with a core diameter from the 10 s to 100 s of microns and a cladding thickness around 10 microns is typically chosen, with larger core diameters providing for easier and more efficient coupling of light into the fiber and a larger emitting area within the brain. Fibers of these dimensions support many (typically thousands) of discrete light propagation modes, and are therefore referred to as ''multimode'' fiber. The core and cladding may be surrounded by a protective ''jacket'' or ''buffer'' layer, which does not contribute to light transmission and is stripped from the fiber before insertion into the brain (Aravanis et al., 2007; Zhang et al., 2010). The interface between the core and cladding reflects light traveling through the core at angles close to the longitudinal axis of the fiber (a phenomenon called ''total internal reflection''), with the difference in refractive indexes between the core and cladding determining the maximum angle of rays that can propagate through the fiber. This relationship is captured by the fiber's numerical aperture (*NA*), which also determines the maximum acceptance angle for incoming light and the maximum exit angle for the output light beam. Fibers with an NA from 0.1 to 0.5 are readily available, giving exit cone angles into brain tissue from 8 to 42 degrees. Since the attenuation with distance from the fiber tip depends partly on the geometric spread of light, fiber NA contributes to the shape of the tissue activated by a given total emitted light power.

Laser light can be efficiently coupled into the fiber with an optical part that focuses the incoming beam onto the end of

the fiber. Couplers that attach directly to the laser head and adjust using small screws are available, but we prefer to rigidly attach the laser and coupler to an optical breadboard, and align the beam using 2 adjustable steering mirrors (Figure 4), which affords faster and more precise alignment. Moreover, this arrangement allows for easy access to the beam path for introducing optical elements such as shutters, beam blocks, filters, beam pick-offs, and power meters. Combining beams from multiple lasers into a single fiber is also easily achieved by the use of a dichroic mirror with the appropriate wavelength cutoff.

Associated enabling technologies for optogenetics in neuroscience: readouts

Optogenetic control has been shown to be compatible with diverse behavioral readouts in organisms ranging from worms and flies to fish and mammals, particularly since the fiberoptic neural interfaces (Adamantidis et al., 2007; Aravanis et al., 2007) are lightweight and flexible enough to allow complex behaviors to be easily carried out in freely moving mammals. One potential challenge to this approach could be a restriction in movement arising from use of a fiber. Nevertheless, analogous issues have been addressed and solved for electrical connectors; in the case of optical hardware, optical commutators allow tracks and arenas to be explored by fiberoptic-coupled mammals exhibiting complex behaviors ranging from rapid circling behavior to place preference and elevated plus maze (Gradinaru et al., 2009; Witten et al., 2010; Tye et al., 2011). Moreover, the latest generation of more light-sensitive and bistable optogenetic tools may enable not only LED-based electrical wire control during behavior, but also free behavior in the complete absence of tethered optical devices (Berndt et al., 2009; Yizhar et al., 2011a). Therefore, as behavioral measures in the setting of optogenetics are relatively straightforward (Nagel et al., 2005; Adamantidis et al., 2007; Huber et al., 2008; Airan et al., 2009; Tsai et al., 2009; Carter et al., 2009; Johansen et al., 2010; Lobo et al., 2010; Witten et al., 2010; Tye et al., 2011) and can be mapped onto the wide range of validated animal behavioral measures present in the literature, here we do not focus on behavioral measures, instead taking note of circuit-level readouts (electrical, optical, and magnetic resonance).

Electrical Readouts

A key advantage of optogenetic stimulation is that true simultaneous electrical recordings can be carried out. Such simultaneous input/output processing is not typically possible with integrated electrical stimulation and electrical recording, due to artifacts associated with electrical stimulation that have stymied both basic systems neuroscience investigations and our understanding of therapeutic brain stimulation modalities such as DBS. Extracellular unit recordings are easily integrated with light stimulation (Gradinaru et al., 2007, 2009), but local field potential recordings with metal electrodes can be confounded with electrical artifacts likely resulting from the direct effects of light and temperature on the recording electrode (Ayling et al., 2009; Cardin et al., 2010). Several simple steps can be taken to assure that LFPs reflect neural activity, including minimization of exposed metal area, use of glass electrodes wherein the conducting wire can be placed further away from the site of recording, and use of nichrome microwires rather than tungsten microelectrodes. Control recordings should be performed in brain regions that contain no opsin-expressing cells, with light at the same wavelength and power density as those used in the experimental recordings within the opsin-expressing region.

When light delivery and electrical recording are integrated into a single device (Gradinaru et al., 2007), the resulting tool is referred to as an "optrode" (Gradinaru et al., 2007, 2009; Zhang et al., 2010). These have ranged from fusion of optical fibers with metallic electrodes (Gradinaru et al., 2007, 2009), to coaxial integrated multielectrode devices (Zhang et al., 2009a, 2009b; Royer et al., 2010), to silicon probes for multi-site recording in awake, behaving animals (Royer et al., 2010). An issue with all of these extracellular methods is that there is no guarantee that recorded spikes are arising from photosensitive cells, rather than from indirectly recruited cells. Normally this is not a concern, and optrode recordings still provide extremely useful feedback on the activity in the local circuit during control that could never be obtained with electrical stimulation. However, care must be taken not to overinterpret (for example) latencies to spiking, which can be highly variable in vivo due to differences in illumination intensity, as predictive of whether a unit is directly or indirectly driven by light. Latencies as long as 10–12 ms or greater are certainly possible for directly driven cells, while conversely latencies as short as 3–4 ms should be possible even for indirectly driven (nonphotosensitive) cells.

Optical Readouts

The concept of all-optical interrogation of neural circuits (Deisseroth et al., 2006; Scanziani and Häusser, 2009) is appealing since spatial distribution and cell-type information can be more readily extracted from imaging data than from electrophysiology. Dye-based imaging has been conducted in combination with optogenetic control in a number of studies, using Ca^{2+} dyes such as fura-2 (Zhang et al., 2007) and Fluo-5F (Zhang and Oertner, 2007), and voltage-sensitive dyes such as RH-155 (Airan et al., 2007, 2009; Zhang et al., 2010). The development of new and improved genetically encoded sensors for neural activity (Lundby et al., 2008; Dreosti et al., 2009; Dreosti and Lagnado, 2011; Lundby et al., 2010; Tian et al., 2009) opens up a new class of possibilities for capitalizing on cell-type-specific readout information that would complement the cell-type-specific play-in of information provided by optogenetics. Although channelrhodopsin action spectra overlap to some extent with the excitation spectra of these fluorophores, one can minimize photoactivation during imaging by minimizing irradiance used to excite the fluorophores, and by using scanning microscopy (confocal or two-photon based).

When using scanning laser microscopy, the rapid ChR kinetics that initially posed challenges for two-photon activation (Rickgauer and Tank, 2009) are actually favorable since Ca^{2+} imaging can be performed by two-photon excitation with minimal photoactivation of ChRs. Indeed, Zhang and Oertner used two-photon imaging of the Ca^{2+} dye Fluo-5F to record dendritic calcium transients evoked with either ChR2 photostimulation or direct current injections in individual neurons in the slice culture preparation (Zhang and Oertner, 2007), while Guo et al. used GCaMP2 in *C.elegans* neurons, using a low wide-field light

power density for imaging GCaMP (488 nm; 0.01 mW/mm^2; Guo et al., 2009) to avoid unwanted photostimulation by the fluorescence excitation light. Finally, spectrotemporal properties of the newer channelrhodopsins offer additional possibilities for combinatorial and all-optical circuit interrogation; red-shifted tools, such as the newly developed C1V1 (Yizhar et al., 2011a) in which peak excitation is further shifted from both the Fura-2 and GCaMP spectra, are even more well suited for integration with Ca^{2+} imaging.

fMRI

Integration of optogenetic control with blood oxygenation level-dependent (BOLD) fMRI readout (ofMRI; Lee et al., 2010) led to the observation that local cortical excitatory neurons could trigger BOLD responses that captured complex dynamics of previously measured sensory-triggered BOLD, providing a causal (rather than the prior correlative) demonstration of sufficiency of coordinated spikes in defined cell types for eliciting the complex dynamics of BOLD signals. It remains to be seen which circuit elements are necessary (rather than sufficient) for distinct phases of BOLD responses in various experimental settings, and this complexity may now be explored with ofMRI (Lee et al., 2010; Leopold, 2010; Desai et al., 2011; Li et al., 2011). Beyond the question of BOLD signal generation, the most significant value of ofMRI will be as a research tool for mapping global impact of defined cells, and perhaps identifying disease-related circuit endophenotypes, in a manner not feasible with microelectrodes, since specific local cells (or specific distant cells defined by axonal wiring) can be directly accessed in the setting of global BOLD mapping. Downstream activation of other networks, regions, cells, and circuit elements is then appropriately dictated by the output of the targeted components.

Outlook

Advances in optogenetics have opened up new landscapes in neuroscience and indeed have already been applied beyond neuroscience to muscle, cardiac, and embryonic stem cells (Arrenberg et al., 2010; Bruegmann et al., 2010; Stirman et al., 2011; Weick et al., 2010; Stroh et al., 2011; Tønnesen et al., 2011). Disease models have also been explored, including for Parkinson's disease, anxiety, retinal degeneration, respiration, cocaine conditioning, and depression (Gradinaru et al., 2009; Covington et al., 2010; Alilain et al., 2008; Kravitz et al., 2010; Witten et al., 2010; Busskamp et al., 2010; Tye et al., 2011). The temporal precision enabled by the use of light along with the single-component microbial opsin strategy is crucial across all fields for delivering a defined event in a defined cell population at a specific time relative to environmental events. Moreover, optogenetic tools may now be selected from a broad and expanding palette (Figure 1) for specific electrical or biochemical effector function, speed, action spectrum, and other properties. Advances in tool functionality and targeting/readout enabling-technologies have allowed the core goal of optogenetics in neuroscience to be achieved: millisecond-scale optical control of defined small-scale events occurring in specified cellular populations while these populations remain embedded and functioning within freely moving mammals or other intact and complex biological systems.

ACKNOWLEDGMENTS

Tools and reagents are freely available at www.optogenetics.org and www.addgene.org, and hands-on optogenetics training courses are available (www.optogenetics.org). We gratefully acknowledge that this research direction was launched with funding beginning July 2004 to K.D. as principal investigator from the National Institutes of Health, from the Stanford Department of Psychiatry, and from the Stanford Department of Bioengineering (www.optogenetics.org/funding). Both this initial microbial opsin work and all subsequent work at Stanford over the years have been financially supported with grants awarded to K.D. from many generous agencies and donors, including from the National Institute of Mental Health, the NIH Director's Pioneer Award, the National Institute on Drug Abuse, the National Institute of Neurological Disorders and Stroke, the National Science Foundation, the Michael J Fox Foundation, the Defense Advanced Research Projects Agency, the California Institute of Regenerative Medicine, and the Coulter, Culpeper, Klingenstein, Whitehall, McKnight, Yu, Woo, Snyder, and Keck Foundations. We thank the many supportive laboratories and members of the Stanford community for collaboration, advice, and equipment-sharing over this time, as well as the many members of the K.D. laboratory in the Clark Center at Stanford over the years. O.Y. is supported by the International Human Frontier Science Program. L.E.F is supported by the Stanford MSTP program, T.J.D. is supported by the Berry Postdoctoral Fellowship, and M.M. is supported by Bio-X, Siebel, and SGF fellowships.

REFERENCES

Adamantidis, A.R., Zhang, F., Aravanis, A.M., Deisseroth, K., and de Lecea, L. (2007). Neural substrates of awakening probed with optogenetic control of hypocretin neurons. Nature *450*, 420–424.

Adesnik, H., and Scanziani, M. (2010). Lateral competition for cortical space by layer-specific horizontal circuits. Nature *464*, 1155–1160.

Airan, R.D., Meltzer, L.A., Roy, M., Gong, Y., Chen, H., and Deisseroth, K. (2007). High-speed imaging reveals neurophysiological links to behavior in an animal model of depression. Science *317*, 819–823.

Airan, R.D., Thompson, K.R., Fenno, L.E., Bernstein, H., and Deisseroth, K. (2009). Temporally precise in vivo control of intracellular signalling. Nature *458*, 1025–1029.

Alilain, W.J., Li, X., Horn, K.P., Dhingra, R., Dick, T.E., Herlitze, S., and Silver, J. (2008). Light-induced rescue of breathing after spinal cord injury. J. Neurosci. *28*, 11862–11870.

Andrasfalvy, B.K., Zemelman, B.V., Tang, J., and Vaziri, A. (2010). Two-photon single-cell optogenetic control of neuronal activity by sculpted light. Proc. Natl. Acad. Sci. USA *107*, 11981–11986.

Aponte, Y., Atasoy, D., and Sternson, S.M. (2011). AGRP neurons are sufficient to orchestrate feeding behavior rapidly and without training. Nat. Neurosci. *14*, 351–355.

Aravanis, A.M., Wang, L.P., Zhang, F., Meltzer, L.A., Mogri, M.Z., Schneider, M.B., and Deisseroth, K. (2007). An optical neural interface: in vivo control of rodent motor cortex with integrated fiberoptic and optogenetic technology. J. Neural Eng. *4*, S143–S156.

Arenkiel, B.R., Peca, J., Davison, I.G., Feliciano, C., Deisseroth, K., Augustine, G.J., Ehlers, M.D., and Feng, G. (2007). In vivo light-induced activation of neural circuitry in transgenic mice expressing channelrhodopsin-2. Neuron *54*, 205–218.

Arrenberg, A.B., Stainier, D.Y., Baier, H., and Huisken, J. (2010). Optogenetic control of cardiac function. Science *330*, 971–974.

Atasoy, D., Aponte, Y., Su, H.H., and Sternson, S.M. (2008). A FLEX switch targets Channelrhodopsin-2 to multiple cell types for imaging and long-range circuit mapping. J. Neurosci. *28*, 7025–7030.

Ayling, O.G., Harrison, T.C., Boyd, J.D., Goroshkov, A., and Murphy, T.H. (2009). Automated light-based mapping of motor cortex by photoactivation of channelrhodopsin-2 transgenic mice. Nat. Methods *6*, 219–224.

Bamann, C., Gueta, R., Kleinlogel, S., Nagel, G., and Bamberg, E. (2010). Structural guidance of the photocycle of channelrhodopsin-2 by an interhelical hydrogen bond. Biochemistry *49*, 267–278.

Banghart, M., Borges, K., Isacoff, E., Trauner, D., and Kramer, R.H. (2004). Light-activated ion channels for remote control of neuronal firing. Nat. Neurosci. *7*, 1381–1386.

Béjà, O., Aravind, L., Koonin, E.V., Suzuki, M.T., Hadd, A., Nguyen, L.P., Jovanovich, S.B., Gates, C.M., Feldman, R.A., Spudich, J.L., et al. (2000). Bacterial rhodopsin: evidence for a new type of phototrophy in the sea. Science *289*, 1902–1906.

Béjà, O., Spudich, E.N., Spudich, J.L., Leclerc, M., and DeLong, E.F. (2001). Proteorhodopsin phototrophy in the ocean. Nature *411*, 786–789.

Benzekhroufa, K., Liu, B., Tang, F., Teschemacher, A.G., and Kasparov, S. (2009a). Adenoviral vectors for highly selective gene expression in central serotonergic neurons reveal quantal characteristics of serotonin release in the rat brain. BMC Biotechnol. *9*, 23.

Benzekhroufa, K., Liu, B.H., Teschemacher, A.G., and Kasparov, S. (2009b). Targeting central serotonergic neurons with lentiviral vectors based on a transcriptional amplification strategy. Gene Ther. *16*, 681–688.

Berndt, A., Yizhar, O., Gunaydin, L.A., Hegemann, P., and Deisseroth, K. (2009). Bi-stable neural state switches. Nat. Neurosci. *12*, 229–234.

Berndt, A., Schoenenberger, P., Mattis, J., Tye, K.M., Deisseroth, K., Hegemann, P., and Oertner, T.G. (2011). High-efficiency channelrhodopsins for fast neuronal stimulation at low light levels. Proc. Natl. Acad. Sci. USA *108*, 7595–7600.

Bernstein, J.G., Han, X., Henninger, M.A., Ko, E.Y., Qian, X., Franzesi, G.T., McConnell, J.P., Stern, P., Desimone, R., and Boyden, E.S. (2008). Prosthetic systems for therapeutic optical activation and silencing of genetically-targeted neurons. Proc. Soc. Photo Opt. Instrum. Eng. *6854*, 68540H.

Bi, A., Cui, J., Ma, Y.P., Olshevskaya, E., Pu, M., Dizhoor, A.M., and Pan, Z.H. (2006). Ectopic expression of a microbial-type rhodopsin restores visual responses in mice with photoreceptor degeneration. Neuron *50*, 23–33.

Blömer, U., Naldini, L., Kafri, T., Trono, D., Verma, I.M., and Gage, F.H. (1997). Highly efficient and sustained gene transfer in adult neurons with a lentivirus vector. J. Virol. *71*, 6641–6649.

Boyden, E.S., Zhang, F., Bamberg, E., Nagel, G., and Deisseroth, K. (2005). Millisecond-timescale, genetically targeted optical control of neural activity. Nat. Neurosci. *8*, 1263–1268.

Brenner, M., Kisseberth, W.C., Su, Y., Besnard, F., and Messing, A. (1994). GFAP promoter directs astrocyte-specific expression in transgenic mice. J. Neurosci. *14*, 1030–1037.

Broekman, M.L., Comer, L.A., Hyman, B.T., and Sena-Esteves, M. (2006). Adeno-associated virus vectors serotyped with AAV8 capsid are more efficient than AAV-1 or -2 serotypes for widespread gene delivery to the neonatal mouse brain. Neuroscience *138*, 501–510.

Brown, M.T., Bellone, C., Mameli, M., Labouèbe, G., Bocklisch, C., Balland, B., Dahan, L., Luján, R., Deisseroth, K., and Lüscher, C. (2010). Drug-driven AMPA receptor redistribution mimicked by selective dopamine neuron stimulation. PLoS ONE *5*, e15870.

Bruegmann, T., Malan, D., Hesse, M., Beiert, T., Fuegemann, C.J., Fleischmann, B.K., and Sasse, P. (2010). Optogenetic control of heart muscle in vitro and in vivo. Nat. Methods *7*, 897–900.

Burger, C., Gorbatyuk, O.S., Velardo, M.J., Peden, C.S., Williams, P., Zolotukhin, S., Reier, P.J., Mandel, R.J., and Muzyczka, N. (2004). Recombinant AAV viral vectors pseudotyped with viral capsids from serotypes 1, 2, and 5 display differential efficiency and cell tropism after delivery to different regions of the central nervous system. Mol. Ther. *10*, 302–317.

Busskamp, V., Duebel, J., Balya, D., Fradot, M., Viney, T.J., Siegert, S., Groner, A.C., Cabuy, E., Forster, V., Seeliger, M., et al. (2010). Genetic reactivation of cone photoreceptors restores visual responses in retinitis pigmentosa. Science *329*, 413–417.

Callaway, E.M. (2008). Transneuronal circuit tracing with neurotropic viruses. Curr. Opin. Neurobiol. *18*, 617–623.

Campagnola, L., Wang, H., and Zylka, M.J. (2008). Fiber-coupled light-emitting diode for localized photostimulation of neurons expressing channelrhodopsin-2. J. Neurosci. Methods *169*, 27–33.

Cardin, J.A., Carlén, M., Meletis, K., Knoblich, U., Zhang, F., Deisseroth, K., Tsai, L.H., and Moore, C.I. (2009). Driving fast-spiking cells induces gamma rhythm and controls sensory responses. Nature *459*, 663–667.

Cardin, J.A., Carlén, M., Meletis, K., Knoblich, U., Zhang, F., Deisseroth, K., Tsai, L.H., and Moore, C.I. (2010). Targeted optogenetic stimulation and recording of neurons in vivo using cell-type-specific expression of Channelrhodopsin-2. Nat. Protoc. *5*, 247–254.

Carter, M.E., Adamantidis, A., Ohtsu, H., Deisseroth, K., and de Lecea, L. (2009). Sleep homeostasis modulates hypocretin-mediated sleep-to-wake transitions. J. Neurosci. *29*, 10939–10949.

Carter, M.E., Yizhar, O., Chikahisa, S., Nguyen, H., Adamantidis, A., Nishino, S., Deisseroth, K., and de Lecea, L. (2010). Tuning arousal with optogenetic modulation of locus coeruleus neurons. Nat. Neurosci. *13*, 1526–1533.

Choi, V.W., McCarty, D.M., and Samulski, R.J. (2005). AAV hybrid serotypes: improved vectors for gene delivery. Curr. Gene Ther. *5*, 299–310.

Chow, B.Y., Han, X., Dobry, A.S., Qian, X., Chuong, A.S., Li, M., Henninger, M.A., Belfort, G.M., Lin, Y., Monahan, P.E., and Boyden, E.S. (2010). High-performance genetically targetable optical neural silencing by light-driven proton pumps. Nature *463*, 98–102.

Chuhma, N., Tanaka, K.F., Hen, R., and Rayport, S. (2011). Functional connectome of the striatal medium spiny neuron. J. Neurosci. *31*, 1183–1192.

Ciocchi, S., Herry, C., Grenier, F., Wolff, S.B., Letzkus, J.J., Vlachos, I., Ehrlich, I., Sprengel, R., Deisseroth, K., Stadler, M.B., et al. (2010). Encoding of conditioned fear in central amygdala inhibitory circuits. Nature *468*, 277–282.

Covington, H.E., 3rd, Lobo, M.K., Maze, I., Vialou, V., Hyman, J.M., Zaman, S., LaPlant, Q., Mouzon, E., Ghose, S., Tamminga, C.A., et al. (2010). Antidepressant effect of optogenetic stimulation of the medial prefrontal cortex. J. Neurosci. *30*, 16082–16090.

Crick, F.H. (1979). Thinking about the brain. Sci. Am. *241*, 219–232.

Cruikshank, S.J., Urabe, H., Nurmikko, A.V., and Connors, B.W. (2010). Pathway-specific feedforward circuits between thalamus and neocortex revealed by selective optical stimulation of axons. Neuron *65*, 230–245.

DeBow, S., and Colbourne, F. (2003). Brain temperature measurement and regulation in awake and freely moving rodents. Methods *30*, 167–171.

Deisseroth, K. (2010). Controlling the brain with light. Sci. Am. *303*, 48–55.

Deisseroth, K. (2011). Optogenetics. Nat. Methods *8*, 26–29.

Deisseroth, K., Feng, G., Majewska, A.K., Miesenböck, G., Ting, A., and Schnitzer, M.J. (2006). Next-generation optical technologies for illuminating genetically targeted brain circuits. J. Neurosci. *26*, 10380–10386.

Depuy, S.D., Kanbar, R., Coates, M.B., Stornetta, R.L., and Guyenet, P.G. (2011). Control of breathing by raphe obscurus serotonergic neurons in mice. J. Neurosci. *31*, 1981–1990.

Desai, M., Kahn, I., Knoblich, U., Bernstein, J., Atallah, H., Yang, A., Kopell, N., Buckner, R.L., Graybiel, A.M., Moore, C.I., and Boyden, E.S. (2011). Mapping brain networks in awake mice using combined optical neural control and fMRI. J. Neurophysiol. *105*, 1393–1405.

Di Pasquale, G., Davidson, B.L., Stein, C.S., Martins, I., Scudiero, D., Monks, A., and Chiorini, J.A. (2003). Identification of PDGFR as a receptor for AAV-5 transduction. Nat. Med. *9*, 1306–1312.

Diester, I., Kaufman, M.T., Mogri, M., Pashaie, R., Goo, W., Yizhar, O., Ramakrishnan, C., Deisseroth, K., and Shenoy, K.V. (2011). An optogenetic toolbox designed for primates. Nat. Neurosci. *14*, 387–397.

Dittgen, T., Nimmerjahn, A., Komai, S., Licznerski, P., Waters, J., Margrie, T.W., Helmchen, F., Denk, W., Brecht, M., and Osten, P. (2004). Lentivirus-based genetic manipulations of cortical neurons and their optical and electrophysiological monitoring in vivo. Proc. Natl. Acad. Sci. USA *101*, 18206–18211.

Dong, J.Y., Fan, P.D., and Frizzell, R.A. (1996). Quantitative analysis of the packaging capacity of recombinant adeno-associated virus. Hum. Gene Ther. *7*, 2101–2112.

Dong, B., Nakai, H., and Xiao, W. (2010). Characterization of genome integrity for oversized recombinant AAV vector. Mol. Ther. *18*, 87–92.

Douglass, A.D., Kraves, S., Deisseroth, K., Schier, A.F., and Engert, F. (2008). Escape behavior elicited by single, channelrhodopsin-2-evoked spikes in zebrafish somatosensory neurons. Curr. Biol. *18*, 1133–1137.

Dreosti, E., and Lagnado, L. (2011). Optical reporters of synaptic activity in neural circuits. Exp. Physiol. *96*, 4–12.

Dreosti, E., Odermatt, B., Dorostkar, M.M., and Lagnado, L. (2009). A genetically encoded reporter of synaptic activity in vivo. Nat. Methods *6*, 883–889.

Elwassif, M.M., Kong, Q., Vazquez, M., and Bikson, M. (2006). Bio-heat transfer model of deep brain stimulation induced temperature changes. Conf. Proc. IEEE Eng. Med. Biol. Soc. *1*, 3580–3583.

Essen, L.O. (2002). Halorhodopsin: light-driven ion pumping made simple? Curr. Opin. Struct. Biol. *12*, 516–522.

Farah, N., Reutsky, I., and Shoham, S. (2007). Patterned optical activation of retinal ganglion cells. Conf. Proc. IEEE Eng. Med. Biol. Soc. *2007*, 6368–6370.

Feldbauer, K., Zimmermann, D., Pintschovius, V., Spitz, J., Bamann, C., and Bamberg, E. (2009). Channelrhodopsin-2 is a leaky proton pump. Proc. Natl. Acad. Sci. USA *106*, 12317–12322.

Fink, D.J., DeLuca, N.A., Goins, W.F., and Glorioso, J.C. (1996). Gene transfer to neurons using herpes simplex virus-based vectors. Annu. Rev. Neurosci. *19*, 265–287.

Freund, T.F. (2003). Interneuron Diversity series: Rhythm and mood in perisomatic inhibition. Trends Neurosci. *26*, 489–495.

Fuhrman, J.A., Schwalbach, M.S., and Stingl, U. (2008). Proteorhodopsins: an array of physiological roles? Nat. Rev. Microbiol. *6*, 488–494.

Gong, S., Doughty, M., Harbaugh, C.R., Cummins, A., Hatten, M.E., Heintz, N., and Gerfen, C.R. (2007). Targeting Cre recombinase to specific neuron populations with bacterial artificial chromosome constructs. J. Neurosci. *27*, 9817–9823.

Gorostiza, P., and Isacoff, E.Y. (2008). Optical switches for remote and noninvasive control of cell signaling. Science *322*, 395–399.

Gourine, A.V., Kasymov, V., Marina, N., Tang, F., Figueiredo, M.F., Lane, S., Teschemacher, A.G., Spyer, K.M., Deisseroth, K., and Kasparov, S. (2010). Astrocytes control breathing through pH-dependent release of ATP. Science *329*, 571–575.

Gradinaru, V., Thompson, K.R., Zhang, F., Mogri, M., Kay, K., Schneider, M.B., and Deisseroth, K. (2007). Targeting and readout strategies for fast optical neural control in vitro and in vivo. J. Neurosci. *27*, 14231–14238.

Gradinaru, V., Thompson, K.R., and Deisseroth, K. (2008). eNpHR: a Natronomonas halorhodopsin enhanced for optogenetic applications. Brain Cell Biol. *36*, 129–139.

Gradinaru, V., Mogri, M., Thompson, K.R., Henderson, J.M., and Deisseroth, K. (2009). Optical deconstruction of parkinsonian neural circuitry. Science *324*, 354–359.

Gradinaru, V., Zhang, F., Ramakrishnan, C., Mattis, J., Prakash, R., Diester, I., Goshen, I., Thompson, K.R., and Deisseroth, K. (2010). Molecular and cellular approaches for diversifying and extending optogenetics. Cell *141*, 154–165.

Greenberg, K.P., Pham, A., and Werblin, F.S. (2011). Differential targeting of optical neuromodulators to ganglion cell soma and dendrites allows dynamic control of center-surround antagonism. Neuron *69*, 713–720.

Grossman, N., Poher, V., Grubb, M.S., Kennedy, G.T., Nikolic, K., McGovern, B., Berlinguer Palmini, R., Gong, Z., Drakakis, E.M., Neil, M.A., et al. (2010). Multi-site optical excitation using ChR2 and micro-LED array. J. Neural Eng. *7*, 16004.

Grossman, N., Nikolic, K., Toumazou, C., and Degenaar, P. (2011). Modeling study of the light stimulation of a neuron cell with channelrhodopsin-2 mutants. IEEE Trans. Biomed. Eng. *58*, 1742–1751.

Gunaydin, L.A., Yizhar, O., Berndt, A., Sohal, V.S., Deisseroth, K., and Hegemann, P. (2010). Ultrafast optogenetic control. Nat. Neurosci. *13*, 387–392.

Guo, Z.V., Hart, A.C., and Ramanathan, S. (2009). Optical interrogation of neural circuits in Caenorhabditis elegans. Nat. Methods *6*, 891–896.

Hägglund, M., Borgius, L., Dougherty, K.J., and Kiehn, O. (2010). Activation of groups of excitatory neurons in the mammalian spinal cord or hindbrain evokes locomotion. Nat. Neurosci. *13*, 246–252.

Han, X., and Boyden, E.S. (2007). Multiple-color optical activation, silencing, and desynchronization of neural activity, with single-spike temporal resolution. PLoS ONE *2*, e299.

Han, X., Qian, X., Bernstein, J.G., Zhou, H.H., Franzesi, G.T., Stern, P., Bronson, R.T., Graybiel, A.M., Desimone, R., and Boyden, E.S. (2009). Millisecond-timescale optical control of neural dynamics in the nonhuman primate brain. Neuron *62*, 191–198.

Haubensak, W., Kunwar, P.S., Cai, H., Ciocchi, S., Wall, N.R., Ponnusamy, R., Biag, J., Dong, H.W., Deisseroth, K., Callaway, E.M., et al. (2010). Genetic dissection of an amygdala microcircuit that gates conditioned fear. Nature *468*, 270–276.

Higley, M.J., and Sabatini, B.L. (2010). Competitive regulation of synaptic Ca2+ influx by D2 dopamine and A2A adenosine receptors. Nat. Neurosci. *13*, 958–966.

Histed, M.H., Bonin, V., and Reid, R.C. (2009). Direct activation of sparse, distributed populations of cortical neurons by electrical microstimulation. Neuron *63*, 508–522.

Hnasko, T.S., Perez, F.A., Scouras, A.D., Stoll, E.A., Gale, S.D., Luquet, S., Phillips, P.E., Kremer, E.J., and Palmiter, R.D. (2006). Cre recombinase-mediated restoration of nigrostriatal dopamine in dopamine-deficient mice reverses hypophagia and bradykinesia. Proc. Natl. Acad. Sci. USA *103*, 8858–8863.

Huber, D., Petreanu, L., Ghitani, N., Ranade, S., Hromádka, T., Mainen, Z., and Svoboda, K. (2008). Sparse optical microstimulation in barrel cortex drives learned behaviour in freely moving mice. Nature *451*, 61–64.

Hull, C., Adesnik, H., and Scanziani, M. (2009). Neocortical disynaptic inhibition requires somatodendritic integration in interneurons. J. Neurosci. *29*, 8991–8995.

Ishizuka, T., Kakuda, M., Araki, R., and Yawo, H. (2006). Kinetic evaluation of photosensitivity in genetically engineered neurons expressing green algae light-gated channels. Neurosci. Res. *54*, 85–94.

Iwai, Y., Honda, S., Ozeki, H., Hashimoto, M., and Hirase, H. (2011). A simple head-mountable LED device for chronic stimulation of optogenetic molecules in freely moving mice. Neurosci. Res. *70*, 124–127.

Jakobsson, J., Ericson, C., Jansson, M., Björk, E., and Lundberg, C. (2003). Targeted transgene expression in rat brain using lentiviral vectors. J. Neurosci. Res. *73*, 876–885.

Johansen, J.P., Hamanaka, H., Monfils, M.H., Behnia, R., Deisseroth, K., Blair, H.T., and LeDoux, J.E. (2010). Optical activation of lateral amygdala pyramidal cells instructs associative fear learning. Proc. Natl. Acad. Sci. USA *107*, 12692–12697.

Kaspar, B.K., Erickson, D., Schaffer, D., Hinh, L., Gage, F.H., and Peterson, D.A. (2002). Targeted retrograde gene delivery for neuronal protection. Mol. Ther. *5*, 50–56.

Kato, S., Inoue, K., Kobayashi, K., Yasoshima, Y., Miyachi, S., Inoue, S., Hanawa, H., Shimada, T., Takada, M., and Kobayashi, K. (2007). Efficient gene transfer via retrograde transport in rodent and primate brains using a human immunodeficiency virus type 1-based vector pseudotyped with rabies virus glycoprotein. Hum. Gene Ther. *18*, 1141–1151.

Kato, S., Kobayashi, K., Inoue, K.I., Kuramochi, M., Okada, T., Yaginuma, H., Morimoto, K., Shimada, T., Takada, M., and Kobayashi, K. (2011). A lentiviral strategy for highly efficient retrograde gene transfer by pseudotyping with fusion envelope glycoprotein. Hum. Gene Ther. *22*, 197–206.

Kätzel, D., Zemelman, B.V., Buetfering, C., Wölfel, M., and Miesenböck, G. (2011). The columnar and laminar organization of inhibitory connections to neocortical excitatory cells. Nat. Neurosci. *14*, 100–107.

Kim, J.M., Hwa, J., Garriga, P., Reeves, P.J., RajBhandary, U.L., and Khorana, H.G. (2005). Light-driven activation of beta 2-adrenergic receptor signaling by a chimeric rhodopsin containing the beta 2-adrenergic receptor cytoplasmic loops. Biochemistry *44*, 2284–2292.

Kleinlogel, S., Feldbauer, K., Dempski, R.E., Fotis, H., Wood, P.G., Bamann, C., and Bamberg, E. (2011). Ultra light-sensitive and fast neuronal activation with the Ca^2+-permeable channelrhodopsin CatCh. Nat. Neurosci. *14*, 513–518.

Kouyama, T., Kanada, S., Takeguchi, Y., Narusawa, A., Murakami, M., and Ihara, K. (2010). Crystal structure of the light-driven chloride pump halorhodopsin from Natronomonas pharaonis. J. Mol. Biol. *396*, 564–579.

Kramer, R.H., Chambers, J.J., and Trauner, D. (2005). Photochemical tools for remote control of ion channels in excitable cells. Nat. Chem. Biol. *1*, 360–365.

Kravitz, A.V., Freeze, B.S., Parker, P.R., Kay, K., Thwin, M.T., Deisseroth, K., and Kreitzer, A.C. (2010). Regulation of parkinsonian motor behaviours by optogenetic control of basal ganglia circuitry. Nature *466*, 622–626.

Kuhlman, S.J., and Huang, Z.J. (2008). High-resolution labeling and functional manipulation of specific neuron types in mouse brain by Cre-activated viral gene expression. PLoS ONE *3*, e2005.

Kumar, M., Keller, B., Makalou, N., and Sutton, R.E. (2001). Systematic determination of the packaging limit of lentiviral vectors. Hum. Gene Ther. *12*, 1893–1905.

Lanyi, J.K., and Oesterhelt, D. (1982). Identification of the retinal-binding protein in halorhodopsin. J. Biol. Chem. *257*, 2674–2677.

Lawlor, P.A., Bland, R.J., Mouravlev, A., Young, D., and During, M.J. (2009). Efficient gene delivery and selective transduction of glial cells in the mammalian brain by AAV serotypes isolated from nonhuman primates. Mol. Ther. *17*, 1692–1702.

Lee, J.H., Durand, R., Gradinaru, V., Zhang, F., Goshen, I., Kim, D.S., Fenno, L.E., Ramakrishnan, C., and Deisseroth, K. (2010). Global and local fMRI signals driven by neurons defined optogenetically by type and wiring. Nature *465*, 788–792.

Leifer, A.M., Fang-Yen, C., Gershow, M., Alkema, M.J., and Samuel, A.D. (2011). Optogenetic manipulation of neural activity in freely moving Caenorhabditis elegans. Nat. Methods *8*, 147–152.

Leopold, D.A. (2010). Neuroscience: fMRI under the spotlight. Nature *465*, 700–701.

Levskaya, A., Weiner, O.D., Lim, W.A., and Voigt, C.A. (2009). Spatiotemporal control of cell signalling using a light-switchable protein interaction. Nature *461*, 997–1001.

Lewis, T.L., Jr., Mao, T., Svoboda, K., and Arnold, D.B. (2009). Myosin-dependent targeting of transmembrane proteins to neuronal dendrites. Nat. Neurosci. *12*, 568–576.

Lewis, T.L., Jr., Mao, T., and Arnold, D.B. (2011). A role for myosin VI in the localization of axonal proteins. PLoS Biol. *9*, e1001021.

Li, X., Gutierrez, D.V., Hanson, M.G., Han, J., Mark, M.D., Chiel, H., Hegemann, P., Landmesser, L.T., and Herlitze, S. (2005). Fast noninvasive activation and inhibition of neural and network activity by vertebrate rhodopsin and green algae channelrhodopsin. Proc. Natl. Acad. Sci. USA *102*, 17816–17821.

Li, N., Downey, J.E., Bar-Shir, A., Gilad, A.A., Walczak, P., Kim, H., Joel, S.E., Pekar, J.J., Thakor, N.V., and Pelled, G. (2011). Optogenetic-guided cortical plasticity after nerve injury. Proc. Natl. Acad. Sci. USA *108*, 8838–8843.

Lilley, C.E., Groutsi, F., Han, Z., Palmer, J.A., Anderson, P.N., Latchman, D.S., and Coffin, R.S. (2001). Multiple immediate-early gene-deficient herpes simplex virus vectors allowing efficient gene delivery to neurons in culture and widespread gene delivery to the central nervous system in vivo. J. Virol. *75*, 4343–4356.

Lima, S.Q., and Miesenböck, G. (2005). Remote control of behavior through genetically targeted photostimulation of neurons. Cell *121*, 141–152.

Lima, S.Q., Hromádka, T., Znamenskiy, P., and Zador, A.M. (2009). PINP: a new method of tagging neuronal populations for identification during in vivo electrophysiological recording. PLoS ONE *4*, e6099.

Lin, J.Y., Lin, M.Z., Steinbach, P., and Tsien, R.Y. (2009). Characterization of engineered channelrhodopsin variants with improved properties and kinetics. Biophys. J. *96*, 1803–1814.

Llewellyn, M.E., Thompson, K.R., Deisseroth, K., and Delp, S.L. (2010). Orderly recruitment of motor units under optical control in vivo. Nat. Med. *16*, 1161–1165.

Lobo, M.K., Covington, H.E., 3rd, Chaudhury, D., Friedman, A.K., Sun, H., Damez-Werno, D., Dietz, D.M., Zaman, S., Koo, J.W., Kennedy, P.J., et al. (2010). Cell type-specific loss of BDNF signaling mimics optogenetic control of cocaine reward. Science *330*, 385–390.

Long, M.A., and Fee, M.S. (2008). Using temperature to analyse temporal dynamics in the songbird motor pathway. Nature *456*, 189–194.

Losonczy, A., Zemelman, B.V., Vaziri, A., and Magee, J.C. (2010). Network mechanisms of theta related neuronal activity in hippocampal CA1 pyramidal neurons. Nat. Neurosci. *13*, 967–972.

Lundby, A., Mutoh, H., Dimitrov, D., Akemann, W., and Knöpfel, T. (2008). Engineering of a genetically encodable fluorescent voltage sensor exploiting fast Ci-VSP voltage-sensing movements. PLoS ONE *3*, e2514.

Lundby, A., Akemann, W., and Knöpfel, T. (2010). Biophysical characterization of the fluorescent protein voltage probe VSFP2.3 based on the voltage-sensing domain of Ci-VSP. Eur. Biophys. J. *39*, 1625–1635.

Madisen, L., Mao, T., Oh, S., Gu, H., Svoboda, K., and Zeng, H. (2010a). Cre driver and responder mice for manipulating neuronal activities in a cell-type selective manner In Society for Neuroscience Meeting (San Diego, CA).

Madisen, L., Zwingman, T.A., Sunkin, S.M., Oh, S.W., Zariwala, H.A., Gu, H., Ng, L.L., Palmiter, R.D., Hawrylycz, M.J., Jones, A.R., et al. (2010b). A robust and high-throughput Cre reporting and characterization system for the whole mouse brain. Nat. Neurosci. *13*, 133–140.

Markakis, E.A., Vives, K.P., Bober, J., Leichtle, S., Leranth, C., Beecham, J., Elsworth, J.D., Roth, R.H., Samulski, R.J., and Redmond, D.E., Jr. (2010). Comparative transduction efficiency of AAV vector serotypes 1-6 in the substantia nigra and striatum of the primate brain. Mol. Ther. *18*, 588–593.

Marshel, J.H., Mori, T., Nielsen, K.J., and Callaway, E.M. (2010). Targeting single neuronal networks for gene expression and cell labeling in vivo. Neuron *67*, 562–574.

Matsuno-Yagi, A., and Mukohata, Y. (1977). Two possible roles of bacteriorhodopsin; a comparative study of strains of Halobacterium halobium differing in pigmentation. Biochem. Biophys. Res. Commun. *78*, 237–243.

Mayford, M., Bach, M.E., Huang, Y.Y., Wang, L., Hawkins, R.D., and Kandel, E.R. (1996). Control of memory formation through regulated expression of a CaMKII transgene. Science *274*, 1678–1683.

Melyan, Z., Tarttelin, E.E., Bellingham, J., Lucas, R.J., and Hankins, M.W. (2005). Addition of human melanopsin renders mammalian cells photoresponsive. Nature *433*, 741–745.

Michel, H., and Oesterhelt, D. (1976). Light-induced changes of the pH gradient and the membrane potential in H. halobium. FEBS Lett. *65*, 175–178.

Miesenböck, G. (2009). The optogenetic catechism. Science *326*, 395–399.

Miyamichi, K., Amat, F., Moussavi, F., Wang, C., Wickersham, I., Wall, N.R., Taniguchi, H., Tasic, B., Huang, Z.J., He, Z., et al. (2011). Cortical representations of olfactory input by trans-synaptic tracing. Nature *472*, 191–196.

Monahan, P.E., and Samulski, R.J. (2000). Adeno-associated virus vectors for gene therapy: more pros than cons? Mol. Med. Today *6*, 433–440.

Moser, E., Mathiesen, I., and Andersen, P. (1993). Association between brain temperature and dentate field potentials in exploring and swimming rats. Science *259*, 1324–1326.

Nagel, G., Ollig, D., Fuhrmann, M., Kateriya, S., Musti, A.M., Bamberg, E., and Hegemann, P. (2002). Channelrhodopsin-1: a light-gated proton channel in green algae. Science *296*, 2395–2398.

Nagel, G., Szellas, T., Huhn, W., Kateriya, S., Adeishvili, N., Berthold, P., Ollig, D., Hegemann, P., and Bamberg, E. (2003). Channelrhodopsin-2, a directly light-gated cation-selective membrane channel. Proc. Natl. Acad. Sci. USA *100*, 13940–13945.

Nagel, G., Brauner, M., Liewald, J.F., Adeishvili, N., Bamberg, E., and Gottschalk, A. (2005). Light activation of channelrhodopsin-2 in excitable cells of Caenorhabditis elegans triggers rapid behavioral responses. Curr. Biol. *15*, 2279–2284.

Nathanson, J.L., Jappelli, R., Scheeff, E.D., Manning, G., Obata, K., Brenner, S., and Callaway, E.M. (2009a). Short Promoters in Viral Vectors Drive Selective Expression in Mammalian Inhibitory Neurons, but do not Restrict Activity to Specific Inhibitory Cell-Types. Front Neural Circuits *3*, 19.

Nathanson, J.L., Yanagawa, Y., Obata, K., and Callaway, E.M. (2009b). Preferential labeling of inhibitory and excitatory cortical neurons by endogenous tropism of adeno-associated virus and lentivirus vectors. Neuroscience *161*, 441–450.

Oesterhelt, D., and Stoeckenius, W. (1971). Rhodopsin-like protein from the purple membrane of Halobacterium halobium. Nat. New Biol. *233*, 149–152.

Oesterhelt, D., and Stoeckenius, W. (1973). Functions of a new photoreceptor membrane. Proc. Natl. Acad. Sci. USA *70*, 2853–2857.

Oh, E., Maejima, T., Liu, C., Deneris, E.S., and Herlitze, S. (2010). Substitution of 5-HT1A receptor signaling by a light-activated G protein-coupled receptor. J. Biol. Chem. *285*, 30825–30836.

Papagiakoumou, E., Anselmi, F., Bègue, A., de Sars, V., Glückstad, J., Isacoff, E.Y., and Emiliani, V. (2010). Scanless two-photon excitation of channelrhodopsin-2. Nat. Methods *7*, 848–854.

Paterna, J.C., Feldon, J., and Büeler, H. (2004). Transduction profiles of recombinant adeno-associated virus vectors derived from serotypes 2 and 5 in the nigrostriatal system of rats. J. Virol. *78*, 6808–6817.

Petreanu, L., Huber, D., Sobczyk, A., and Svoboda, K. (2007). Channelrhodopsin-2-assisted circuit mapping of long-range callosal projections. Nat. Neurosci. *10*, 663–668.

Petreanu, L., Mao, T., Sternson, S.M., and Svoboda, K. (2009). The subcellular organization of neocortical excitatory connections. Nature *457*, 1142–1145.

Qing, K., Mah, C., Hansen, J., Zhou, S., Dwarki, V., and Srivastava, A. (1999). Human fibroblast growth factor receptor 1 is a co-receptor for infection by adeno-associated virus 2. Nat. Med. *5*, 71–77.

Racker, E., and Stoeckenius, W. (1974). Reconstitution of purple membrane vesicles catalyzing light-driven proton uptake and adenosine triphosphate formation. J. Biol. Chem. *249*, 662–663.

Ren, J., Qin, C., Hu, F., Tan, J., Qiu, L., Zhao, S., Feng, G., and Luo, M. (2011). Habenula "cholinergic" neurons co-release glutamate and acetylcholine and activate postsynaptic neurons via distinct transmission modes. Neuron *69*, 445–452.

Rickgauer, J.P., and Tank, D.W. (2009). Two-photon excitation of channelrhodopsin-2 at saturation. Proc. Natl. Acad. Sci. USA *106*, 15025–15030.

Ritter, E., Stehfest, K., Berndt, A., Hegemann, P., and Bartl, F.J. (2008). Monitoring light-induced structural changes of Channelrhodopsin-2 by UV-visible and Fourier transform infrared spectroscopy. J. Biol. Chem. *283*, 35033–35041.

Royer, S., Zemelman, B.V., Barbic, M., Losonczy, A., Buzsáki, G., and Magee, J.C. (2010). Multi-array silicon probes with integrated optical fibers: light-assisted perturbation and recording of local neural circuits in the behaving animal. Eur. J. Neurosci. *31*, 2279–2291.

Ryu, M.H., Moskvin, O.V., Siltberg-Liberles, J., and Gomelsky, M. (2010). Natural and engineered photoactivated nucleotidyl cyclases for optogenetic applications. J. Biol. Chem. *285*, 41501–41508.

Sasaki, J., Brown, L.S., Chon, Y.S., Kandori, H., Maeda, A., Needleman, R., and Lanyi, J.K. (1995). Conversion of bacteriorhodopsin into a chloride ion pump. Science *269*, 73–75.

Sato, M., Kubo, M., Aizawa, T., Kamo, N., Kikukawa, T., Nitta, K., and Demura, M. (2005). Role of putative anion-binding sites in cytoplasmic and extracellular channels of Natronomonas pharaonis halorhodopsin. Biochemistry *44*, 4775–4784.

Scanziani, M., and Häusser, M. (2009). Electrophysiology in the age of light. Nature *461*, 930–939.

Scharf, B., and Engelhard, M. (1994). Blue halorhodopsin from Natronobacterium pharaonis: wavelength regulation by anions. Biochemistry *33*, 6387–6393.

Schobert, B., and Lanyi, J.K. (1982). Halorhodopsin is a light-driven chloride pump. J. Biol. Chem. *257*, 10306–10313.

Schultheis, C., Liewald, J.F., Bamberg, E., Nagel, G., and Gottschalk, A. (2011). Optogenetic long-term manipulation of behavior and animal development. PLoS ONE *6*, e18766.

Shoham, S. (2010). Optogenetics meets optical wavefront shaping. Nat. Methods *7*, 798–799.

Sohal, V.S., Zhang, F., Yizhar, O., and Deisseroth, K. (2009). Parvalbumin neurons and gamma rhythms enhance cortical circuit performance. Nature *459*, 698–702.

Soudais, C., Skander, N., and Kremer, E.J. (2004). Long-term in vivo transduction of neurons throughout the rat CNS using novel helper-dependent CAV-2 vectors. FASEB J. *18*, 391–393.

Stierl, M., Stumpf, P., Udwari, D., Gueta, R., Hagedorn, R., Losi, A., Gärtner, W., Petereit, L., Efetova, M., Schwarzel, M., et al. (2011). Light modulation of cellular cAMP by a small bacterial photoactivated adenylyl cyclase, bPAC, of the soil bacterium Beggiatoa. J. Biol. Chem. *286*, 1181–1188.

Stirman, J.N., Crane, M.M., Husson, S.J., Wabnig, S., Schultheis, C., Gottschalk, A., and Lu, H. (2011). Real-time multimodal optical control of neurons and muscles in freely behaving Caenorhabditis elegans. Nat. Methods *8*, 153–158.

Stroh, A., Tsai, H.C., Wang, L.P., Zhang, F., Kressel, J., Aravanis, A., Santhanam, N., Deisseroth, K., Konnerth, A., and Schneider, M.B. (2011). Tracking stem cell differentiation in the setting of automated optogenetic stimulation. Stem Cells *29*, 78–88.

Stuber, G.D., Hnasko, T.S., Britt, J.P., Edwards, R.H., and Bonci, A. (2010). Dopaminergic terminals in the nucleus accumbens but not the dorsal striatum corelease glutamate. J. Neurosci. *30*, 8229–8233.

Summerford, C., and Samulski, R.J. (1998). Membrane-associated heparan sulfate proteoglycan is a receptor for adeno-associated virus type 2 virions. J. Virol. *72*, 1438–1445.

Summerford, C., Bartlett, J.S., and Samulski, R.J. (1999). AlphaVbeta5 integrin: a co-receptor for adeno-associated virus type 2 infection. Nat. Med. *5*, 78–82.

Tan, W., Janczewski, W.A., Yang, P., Shao, X.M., Callaway, E.M., and Feldman, J.L. (2008). Silencing preBötzinger complex somatostatin-expressing neurons induces persistent apnea in awake rat. Nat. Neurosci. *11*, 538–540.

Tan, W., Pagliardini, S., Yang, P., Janczewski, W.A., and Feldman, J.L. (2010). Projections of preBötzinger complex neurons in adult rats. J. Comp. Neurol. *518*, 1862–1878.

Thyagarajan, S., van Wyk, M., Lehmann, K., Löwel, S., Feng, G., and Wässle, H. (2010). Visual function in mice with photoreceptor degeneration and transgenic expression of channelrhodopsin 2 in ganglion cells. J. Neurosci. *30*, 8745–8758.

Tian, L., Hires, S.A., Mao, T., Huber, D., Chiappe, M.E., Chalasani, S.H., Petreanu, L., Akerboom, J., McKinney, S.A., Schreiter, E.R., et al. (2009). Imaging neural activity in worms, flies and mice with improved GCaMP calcium indicators. Nat. Methods *6*, 875–881.

Toni, N., Laplagne, D.A., Zhao, C., Lombardi, G., Ribak, C.E., Gage, F.H., and Schinder, A.F. (2008). Neurons born in the adult dentate gyrus form functional synapses with target cells. Nat. Neurosci. *11*, 901–907.

Tønnesen, J., Sørensen, A.T., Deisseroth, K., Lundberg, C., and Kokaia, M. (2009). Optogenetic control of epileptiform activity. Proc. Natl. Acad. Sci. USA *106*, 12162–12167.

Tønnesen, J., Parish, C.L., Sørensen, A.T., Andersson, A., Lundberg, C., Deisseroth, K., Arenas, E., Lindvall, O., and Kokaia, M. (2011). Functional integration of grafted neural stem cell-derived dopaminergic neurons monitored by optogenetics in an in vitro Parkinson model. PLoS ONE *6*, e17560.

Towne, C., Schneider, B.L., Kieran, D., Redmond, D.E., Jr., and Aebischer, P. (2010). Efficient transduction of non-human primate motor neurons after intramuscular delivery of recombinant AAV serotype 6. Gene Ther. *17*, 141–146.

Tsai, H.C., Zhang, F., Adamantidis, A., Stuber, G.D., Bonci, A., de Lecea, L., and Deisseroth, K. (2009). Phasic firing in dopaminergic neurons is sufficient for behavioral conditioning. Science *324*, 1080–1084.

Tsunoda, S.P., and Hegemann, P. (2009). Glu 87 of channelrhodopsin-1 causes pH-dependent color tuning and fast photocurrent inactivation. Photochem. Photobiol. *85*, 564–569.

Tye, K.M., Prakash, R., Kim, S.Y., Fenno, L.E., Grosenick, L., Zarabi, H., Thompson, K.R., Gradinaru, V., Ramakrishnan, C., and Deisseroth, K. (2011). Amygdala circuitry mediating reversible and bidirectional control of anxiety. Nature *471*, 358–362.

Váró, G., Brown, L.S., Lakatos, M., and Lanyi, J.K. (2003). Characterization of the photochemical reaction cycle of proteorhodopsin. Biophys. J. *84*, 1202–1207.

Vo-Dinh T., ed. (2003). Biomedical Photonics Handbook (Boca Raton, FL: CRC Press).

Volgraf, M., Gorostiza, P., Numano, R., Kramer, R.H., Isacoff, E.Y., and Trauner, D. (2006). Allosteric control of an ionotropic glutamate receptor with an optical switch. Nat. Chem. Biol. *2*, 47–52.

Wang, H., Peca, J., Matsuzaki, M., Matsuzaki, K., Noguchi, J., Qiu, L., Wang, D., Zhang, F., Boyden, E., Deisseroth, K., et al. (2007). High-speed mapping of synaptic connectivity using photostimulation in Channelrhodopsin-2 transgenic mice. Proc. Natl. Acad. Sci. USA *104*, 8143–8148.

Wang, H., Sugiyama, Y., Hikima, T., Sugano, E., Tomita, H., Takahashi, T., Ishizuka, T., and Yawo, H. (2009). Molecular determinants differentiating photocurrent properties of two channelrhodopsins from chlamydomonas. J. Biol. Chem. *284*, 5685–5696.

Watson, B.O., Nikolenko, V., and Yuste, R. (2009). Two-photon imaging with diffractive optical elements. Front Neural Circuits *3*, 6.

Weick, J.P., Johnson, M.A., Skroch, S.P., Williams, J.C., Deisseroth, K., and Zhang, S.C. (2010). Functional control of transplantable human ESC-derived neurons via optogenetic targeting. Stem Cells *28*, 2008–2016.

Wen, L., Wang, H., Tanimoto, S., Egawa, R., Matsuzaka, Y., Mushiake, H., Ishizuka, T., and Yawo, H. (2010). Opto-current-clamp actuation of cortical neurons using a strategically designed channelrhodopsin. PLoS ONE *5*, e12893.

Witten, I.B., Lin, S.C., Brodsky, M., Prakash, R., Diester, I., Anikeeva, P., Gradinaru, V., Ramakrishnan, C., and Deisseroth, K. (2010). Cholinergic interneurons control local circuit activity and cocaine conditioning. Science *330*, 1677–1681.

Wu, Y.I., Frey, D., Lungu, O.I., Jaehrig, A., Schlichting, I., Kuhlman, B., and Hahn, K.M. (2009). A genetically encoded photoactivatable Rac controls the motility of living cells. Nature *461*, 104–108.

Yaroslavsky, A.N., Schulze, P.C., Yaroslavsky, I.V., Schober, R., Ulrich, F., and Schwarzmaier, H.J. (2002). Optical properties of selected native and coagulated human brain tissues in vitro in the visible and near infrared spectral range. Phys. Med. Biol. *47*, 2059–2073.

Yazawa, M., Sadaghiani, A.M., Hsueh, B., and Dolmetsch, R.E. (2009). Induction of protein-protein interactions in live cells using light. Nat. Biotechnol. *27*, 941–945.

Yizhar, O., Fenno, L., Prigge, M., Davidson, T.J., O'Shea, D.J., Sohal, V.S., Goshen, I., Finkelstein, J., Paz, J., Stehfest, K., et al. (2011a). Neocortical excitation/inhibition balance in social dysfunction and information processing. Nature, submitted.

Yizhar, O., Fenno, L., Zhang, F., Hegemann, P., and Diesseroth, K. (2011b). Microbial opsins: a family of single-component tools for optical control of neural activity. Cold Spring Harb. Protoc. *2011*, top102.

Zariwala, H.A., Madisen, L., Ahrens, K.F., Bernard, A., Lein, E.S., Jones, A.R., and Zeng, H. (2011). Visual tuning properties of genetically identified layer 2/3 neuronal types in the primary visual cortex of cre-transgenic mice. Front Syst Neurosci *4*, 162.

Zemelman, B.V., Lee, G.A., Ng, M., and Miesenböck, G. (2002). Selective photostimulation of genetically chARGed neurons. Neuron *33*, 15–22.

Zemelman, B.V., Nesnas, N., Lee, G.A., and Miesenbock, G. (2003). Photochemical gating of heterologous ion channels: remote control over genetically designated populations of neurons. Proc. Natl. Acad. Sci. USA *100*, 1352–1357.

Zhang, F. (2008). Fast optical neural circuit interrogation technology: development and applications. Larry Katz Memorial Lecture. In Cold Spring Harbor Laboratory Meeting on Neuronal Circuits: From Structure to Function (Cold Spring Harbor).

Zhang, Y.P., and Oertner, T.G. (2007). Optical induction of synaptic plasticity using a light-sensitive channel. Nat. Methods *4*, 139–141.

Zhang, F., Wang, L.P., Boyden, E.S., and Deisseroth, K. (2006). Channelrhodopsin-2 and optical control of excitable cells. Nat. Methods *3*, 785–792.

Zhang, F., Wang, L.P., Brauner, M., Liewald, J.F., Kay, K., Watzke, N., Wood, P.G., Bamberg, E., Nagel, G., Gottschalk, A., and Deisseroth, K. (2007). Multimodal fast optical interrogation of neural circuitry. Nature *446*, 633–639.

Zhang, F., Prigge, M., Beyrière, F., Tsunoda, S.P., Mattis, J., Yizhar, O., Hegemann, P., and Deisseroth, K. (2008). Red-shifted optogenetic excitation: a tool for fast neural control derived from Volvox carteri. Nat. Neurosci. *11*, 631–633.

Zhang, J., Laiwalla, F., Kim, J.A., Urabe, H., Van Wagenen, R., Song, Y.K., Connors, B.W., and Nurmikko, A.V. (2009a). A microelectrode array incorporating an optical waveguide device for stimulation and spatiotemporal electrical recording of neural activity. Conf. Proc. IEEE Eng. Med. Biol. Soc. *2009*, 2046–2049.

Zhang, J., Laiwalla, F., Kim, J.A., Urabe, H., Van Wagenen, R., Song, Y.K., Connors, B.W., Zhang, F., Deisseroth, K., and Nurmikko, A.V. (2009b). Integrated device for optical stimulation and spatiotemporal electrical recording of neural activity in light-sensitized brain tissue. J. Neural Eng. *6*, 055007.

Zhang, F., Gradinaru, V., Adamantidis, A.R., Durand, R., Airan, R.D., de Lecea, L., and Deisseroth, K. (2010). Optogenetic interrogation of neural circuits: technology for probing mammalian brain structures. Nat. Protoc. *5*, 439–456.

Zhao, S., Cunha, C., Zhang, F., Liu, Q., Gloss, B., Deisseroth, K., Augustine, G.J., and Feng, G. (2008). Improved expression of halorhodopsin for light-induced silencing of neuronal activity. Brain Cell Biol. *36*, 141–154.

Zhao, S., Qiu, L., Ting, J., Tan, J., Gloss, B., Deisseroth, K., Luo, M., and Feng, G. (2010). Cell-type specific optogenetic mice for dissecting neural circuitry function. Program No. 412.8/OOO36. 2010 Neuroscience Meeting Planner Online. San Diego, CA: Society for Neuroscience.

Zimmermann, D., Zhou, A., Kiesel, M., Feldbauer, K., Terpitz, U., Haase, W., Schneider-Hohendorf, T., Bamberg, E., and Sukhorukov, V.L. (2008). Effects on capacitance by overexpression of membrane proteins. Biochem. Biophys. Res. Commun. *369*, 1022–1026.